2007-10-09

A Generalized Two-Dimensional Model to Reconstruct the Impact Phase in Automobile Collisions

Regis Agenor David
Brigham Young University - Provo

A GENERALIZED TWO-DIMENSIONAL MODEL TO RECONSTRUCT THE IMPACT PHASE IN AUTOMOBILE COLLISIONS

by

Regis A. David

A thesis submitted to the faculty of

Brigham Young University

in partial fulfillment of the requirements for the degree of

Master of Science

Department of Mechanical Engineering

Brigham Young University

December 2007

BRIGHAM YOUNG UNIVERSTITY

GRADUATE COMMITTEE APPROVAL

Of a thesis submitted by

Regis A. David

This thesis has been read by each member of the following graduate committee and by majority vote has been found to be satisfactory.

_____	_____
Date	Craig C. Smith, Chair
_____	_____
Date	Brian D. Jensen
_____	_____
Date	Deryl O. Snyder

BRIGHAM YOUNG UNIVERSITY

As chair of the candidate's graduate committee, I have read the thesis of Regis A. David in its final form and have found that (1) its format, citations, and bibliographical style are consistent and acceptable and fulfill university and department style requirements; (2) its illustrative materials including figures, tables, and charts are in place; and (3) the final manuscript is satisfactory to the graduate committee and is ready for submission to the university library.

_____	_____
Date	Craig C. Smith Chair, Graduate Committee

Accepted for the Department

_____	_____
Date	Matthew R. Jones Graduate Coordinator

Accepted for the College

_____	_____
Date	Alan R. Parkinson Dean, The A. Fulton College of Engineering and Technology

ABSTRACT

A GENERALIZED TWO-DIMENSIONAL MODEL TO RECONSTRUCT THE IMPACT PHASE IN AUTOMOBILE COLLISIONS

Regis A. David

Department of Mechanical Engineering

Master of Science

Automobile accident reconstruction has been facilitated by the development of computer based modules to allow evaluation of evidence gathered at the accident scenes. Although the computer modules are based in fundamental physical laws, an understanding of these laws by the user is required for proper application of the computer model in a given accident scenario.

Vehicle collision analysis techniques generally separate the collision into three phases: pre-impact, impact, and post impact. The intent of the research is to provide a generalized model to reconstruct two dimensional impact problems in the area of accident reconstruction. There are currently two modeling techniques used to reconstruct the impact phase: the first technique relying exclusively on impulse-momentum theory

coupled with friction and restitution, while the second method combines impulse momentum with a relationship between crush geometry and energy loss. Because each method requires very different inputs, the literature would have us believe that both methods are different. We will show that both methods are derived using the same fundamental physical principles and for any given accident scenario, both methods will provide identical results. Each method will be presented in the form of a MathCAD spread sheet that will allow the user to reconstruct a wide variety of accidents controlling just a few parameters (i.e. mass, rotational inertia, angle of approach, etc…). Both methods will provide step by step graphical representation to assure a solid approach to physical fundamentals. The governing equations to the generalized energy approach will be non-dimensionalized and used to define all of the changes in energy (i.e. also referred to as an impulse in power) as a function of a characteristic velocity. Finally, different methods to consistently determine the direction of the force will be presented when additional information from the accident scene is provided.

ACKNOWLEDGMENTS

I would like to thank all of the professors at BYU for their encouragements in pursuing an advanced degree.

Dr. Craig Smith has been the most helpful in this process. He provided me with an ability to further my understanding of mechanical system dynamics. He proposed this project and has been a great support. I am grateful for his expertise in the subject area. I have thoroughly enjoyed working with him and I have great admiration for him.

Dr. Charles Warner and Collision Safety Engineering, Inc were kind enough to let me use their facility and have been extremely helpful with their knowledge and insights.

My parents have always been an immense influence in my scholastic pursuit. They have provided a way for me to attend College and later on University. They have always been supportive in my choices. I am grateful for their love.

Finally, I would also like to recognize the influence of my older siblings who have obtained advanced degrees and for the effect they had on me.

TABLE OF CONTENTS

CHAPTER 1: INTRODUCTION 1
Introduction 1
Literature Review 2
Objective 7
Approach 8
Nomenclature 8

CHAPTER 2: ANALYTYCAL MODEL OF THE SYSTEM 11
Objective 11
The Model 12
Impulse in Power 19

CHAPTER 3: NON-DIMENSIONAL MODEL OF THE SYSTEM 21
Objective 21
Momentum Exchange 21
Energy Exchange 24

CHAPTER 4: ENERGY APROACH USING MATHCAD 29
Objective 29
The Momentum Module 30
The Energy Module 35
Pinned-Joint Constraint 44
Velocity Ratio 50

CHAPTER 5: PHYSICAL CONSTRAINT AND BOUNDARY CONDITION ... 53
Objective 53
Pinned-Joint Constraint with Restitution 53
Sideswipe Impact 57
Sideswipe Impact with Restitution 63
Plots of Velocities as a function of θ_E from 0 to 360 degrees 64

CHAPTER 6: CONCLUSION 69
Objective of the Paper 69
New Insights for Both Approaches 69
Contributions 69

REFERENCES 71

LIST OF FIGURES

2-1	Non-central frontal collision ……	12
2-2	Non-central collision modeling ……	13
2-3	A 0 junction ……	14
2-4	Identity 0 junction ……	14
2-5	Equivalent inertial mass of vehicle 1 ……	15
2-6	Effective mass of the system ……	16
3-1	Plot of the non-dimensional energy changes vs. initial velocity of vehicle 1	27
4-1	Graphical representation of vehicle 1 ……	31
4-2	Graphical representation of vehicle 2 ……	32
4-3	Frontal damage profile for vehicle 1 ……	36
4-4	Plot of Residual Crush v.s. Impact Speed for Frontal Barrier Tests ……	40
4-5	Direction of the force (Vehicle 1) ……	42
4-6	Direction of the force (Vehicle 2) ……	43
4-7	Translational components ……	45
4-8	Closing Velocity when $\theta = -120$ (a), and $\theta = 180$ (b) ……	49
5-1	Representation of the separating velocity in the momentum module …	58
5-2	Plot of velocities difference as a function of θ_E from 0 to 360 degrees …	66
5-3	Plot of velocities as a function of θ_E from 0 to 360 degrees ……	67

LIST OF TABLES

4-1	Input for momentum module	33
4-2	Output from momentum module	34
4-3	Input for energy module	48
4-4	Output from energy module	48
5-1	Input for momentum module with $\varepsilon = 0.15$	55
5-2	Output from momentum module for $\varepsilon = 0.15$	56
5-3	Input for energy module with $\varepsilon = 0.15$	56
5-4	Output from energy module for $\varepsilon = 0.15$	57
5-5	Input for momentum module for $\mu = 80\% \mu_o$	60
5-6	Output from momentum module for $\mu = 80\% \mu_o$	62
5-7	Input for energy module	62
5-8	Output from energy module	63
5-9	Output from momentum module for $\varepsilon = 0.2$ and $\mu = 80\% \mu_o$	64
5-10	Output from energy module for $\varepsilon = 0.2$	64

CHAPTER 1: INTRODUCTION

Introduction

Motor vehicle crashes are reconstructed by several types of agencies. For example, the Federal Government reconstructs accidents for statistical purposes and to fund or perform research on behalf of the general public. Vehicle manufacturers reconstruct accidents to help design safer cars and restraint systems. Insurance companies and litigators use consultants to reconstruct crashes to determine liability. Finally, law enforcement personnel reconstruct accidents to determine if any laws were violated. Computer programs have been used to analyze motor vehicle accidents since the early seventies [8]. These programs were developed by large research institutes and were used by engineers and scientists who developed them. With the introduction of the personal computer in the early eighties, these programs have become available for use by the general accident investigation community. Just as the level of skill varies among investigators, the level of understanding of how the program works also varies. When properly used, these computer programs are an invaluable accident investigation tool. When misused, these programs can produce erroneous results and a misconception of what actually occurred during the accident [8].

Literature Review

The literature review will begin by defining several types of computer programs popular within the accident investigation community. The five most popular computer programs have been categorized as follow: general analysis, vehicle dynamics, impact dynamics, human dynamics, and photogrammetry. [8] gives a thorough evaluation of all five computer types, including basic assumptions, limitations, application and how they can be misused.

As with all forms of analysis, accurate input data are required to obtain accurate results. As mentioned above, each of these five types of computer programs performs a specific task. The one of interest for this work is the third type. Impact dynamics programs are used for studying accidents which include vehicle-to-vehicle or vehicle-to-barrier collisions. Although these models concentrate on the impact phase, some of them also analyze the pre-impact and/or post-impact phases as well. The primary purpose of these programs is to estimate impact speed and delta-Vs (change in velocity). Some of the most popular impact dynamics programs and their theories will be presented here. The first (CRASH) uses an approach different than the others. For information on all other programs, refer to the existing literature.

CRASH - Calspan Reconstruction of Accident Speeds on the Highway- in the form of CRASH3 and its predecessor CRASH2 has probably been utilized more times than any other reconstruction program. Originally, The National Highway Traffic Safety Administration (NHTSA) funded the development of CRASH as a way to compare the CRASH model to crash tests and establish accuracy and sensitivity in the model for the use in statistical analysis of accident severity [26]. CRASH uses an approach that

combines conservation of momentum and conservation of energy. The procedure, which is based upon the method proposed by Campbell [5], requires comparative crash test data and crush measurements taken from the accident vehicles. This "damage only" option of the program gives an estimate of the vehicles delta-V, assuming the analyst is able to estimate the principal direction of force (*PDOF*) relative to the road surface, the point of application of the force resultant on the cars and the distance offset between the force and the CG of each vehicle and the energy dissipated by crush. CRASH does this by interpreting vehicle properties (mass, rotational inertia, etc…), vehicle heading, crush profile and *PDOF* relative to each vehicle [17]. The momentum calculation uses the assumption that there is a common velocity achieved at one point in the mutual crush zone (or common CG velocity in the case of a collinear collision). The centroid of the crush volume of each car is selected as the common point. The collision force is directed along the line of action which passes though the common point and has the direction specified by the user. Thus the user must determine the principal direction of force from an estimation of the damaged vehicle. Because the direction of the impulse (time integral of the force) is parallel to the momentum change, the direction of the delta-V vector is specified by *PDOF*. As imagined, pre-specification of the *PDOF* angles is difficult due to the complex buckling pattern of the vehicle structure and the intricate displacement of metal parts during the impact. Therefore, the analyst may only be able to give a range of possibilities which will produce a range of delta-V. When the accuracy and sensitivity of the damage option in CRASH was studied by NHTSA [22], it was reported that estimation of the *PDOF* was the most critical measurement reported by field investigators, accounting for 18 % error in vehicle delta-V. As a rule of thumb, it is

always appropriate to compare your results with other momentum based programs. Perhaps, the central disadvantage of the "damage only" approach is that it can only yield information regarding the changes in velocity during the collision. Additional information must be specified in order to obtain initial and final velocities.

SMAC - Simulation Model of Automobile Collision- produces an accident simulation according to the laws of physics. The program uses the investigator's estimates for the initial vehicle speeds, along with vehicle data, tire/road friction data and driver control (acceleration, braking and steering) table. The output is a simulated vehicle trajectory and damage profile for each vehicle. The objective is to find a set of initial speeds which produces the best match between the simulated and actual vehicle trajectories and damage profiles. One of SMAC's most useful applications is theory testing [8]. Multiple scenarios can be simulated and the closest to the actual trajectories and damage is selected. SMAC requires force-deflection information for each vehicle, which is sometimes difficult to obtain or unknown at the level of detail required.

IMPAC - Impact Momentum of a Planar Angled Collision is intended to provide a very straightforward and simple analysis of angled collision. It is similar to CRASH in that it uses scene data as input. Like SMAC, it requires estimate of initial speeds as input prior to impact data and uses these estimates to predict the separation condition (Velocity and direction) [8]. It deals only with momentum transfer and does not directly use crush energy.

PC-CRASH - A Momentum-Based Accident reconstruction Program uses a 2D or 3D dimensional impact model that relies on restitution rather than vehicle crush or stiffness coefficients. This model assumes an exchange of the impact forces within an

infinitely small time step at a single point called the impulse point. Instead of resolving the impact forces over time, only the integral of the force-time curve (the impulse) is considered. This model contains the means to calculate impacts in which a common velocity is reached by the contacting areas of the two vehicles (full impact) and impacts where no common velocity is reached (sideswipe impact). The crash model allows the calculation of the post impact parameters after the definition of the pre-impact phase (speeds and positions) [23].

Other 3D programs created by Engineering Dynamics Corp are also available to the public and their abilities have been compared with that of PC-CRASH [9]. Since the focus of this thesis is not on 3D models, the reader is left to research on his own for further knowledge.

Recently, Raymond M. Brach and R. Matthew Brach published a book called "Vehicle Accident Analysis and Reconstruction Methods" [4]. The book is one of many published on the topic of accident reconstruction. "With some notable exceptions, many of these books are works devoted to how the authors and perhaps a few colleagues used intuition and insight to decide how they thought an accident happened. In a few cases, these books are collections of case histories; usually presentation of one view of the events" [4]. In contrast, the authors of "Vehicle Accident Analysis and Reconstruction Methods" affirm that their book is one of methods [4]. In Chapter 6, the authors developed a set of equations also known as the planar point-mass impulse-momentum equations. For any two bodies placed in a fixed reference coordinate system (x-y axes), there exists a normal and tangential set of coordinate axis (n-t axes) dependant upon the geometry of the contact oriented with respect to the (x,y) system by an angle. The (n-t)

axis pair is chosen so that the normal axis is perpendicular to the assumed contact surface. The equations mentioned earlier are Newton's law of impulse and momentum applied in the (n-t) system. In addition, a coefficient of restitution relating the final relative normal rebound velocity to the initial relative normal velocity and an impulse ratio relating the tangential impulse component to the normal impulse component are introduced. The impulse ratio mentioned above is not a coefficient of friction but can be related to one. In fact it is the approach used in PC-CRASH [23] and also defined in an SAE paper written by Gregory C. Smith [21]. In order to apply rotational momentum, two more equations are added and the theory takes on new name: "Planar Impact Mechanics". Given certain information, the planar impact mechanics model provides a way of calculating the final velocity components and impulse components of two colliding vehicles. The input information can be grouped into four physical categories: the initial velocity components (translational and rotational), the physical properties of the vehicles (masses and rotational inertias), the orientation angles (headings) and the collision-damage characteristics (Point of contact, orientation of n-t, restitution coefficient, impulse ratio). The coefficient of restitution and impulse ratio relate to the level of energy loss. Indeed, when the coefficient of restitution is 1 and the impulse ratio is 0, the collision is a perfectly elastic and frictionless collision with no energy lost. When the coefficient of restitution is 0 and the impulse ratio is at a maximum (that is when the relative tangential separating velocity is 0) the energy loss is a maximum. To apply planar impact mechanics, it is necessary to make assumptions. One is that a single, intervehicular crush surface can be represented by one that lies in a vertical plane and a common point exists that represents the point of application of the intervehicular impulse.

That point represents an average of the distance from the center of gravity to the crushing region over space and time. Whatever method is used, judgment of the analysist is necessary [4].

Objective

The objectives of this work are as follows: First, this work will provide a more generalized energy model approach to reconstruct two-dimensional impact problems in the area of accident reconstruction. This energy model will show that the same closed form solution given in CRASH3 can be obtained using an approach that does not require the representation of a linear spring (crush of the car modeled as a linear spring) and does not assume simple harmonic motion as a trivial solution. We will establish a consistent sign convention that relates the physical phenomena to the modeled system. Terms pertinent to this approach will be defined and the governing equations will be non-dimensionalized and used to define all of the changes in momentum and energy as a function of a characteristic velocity. In addition, we will derive an expression for the average velocity experienced by each vehicle during impact as a function of the change in energy.

We will verify that although both methods require very different inputs, they are derived using the same fundamental physical principals and for any given accident scenario, including sideswipe impact, they will provide identical results. We will extend the solution provided in CRASH3 by calculating the velocity prior and after impact for both vehicles. We will also present different methods to consistently determine the direction of the force when additional information from the accident scene is provided.

Approach

The generalized energy model will be derived using a bond-graph to represent the planar impact collision between two vehicles. Each method will be presented in the form of a MathCAD spread sheet that will allow the user to reconstruct a wide variety of accidents controlling just a few parameters (i.e. mass, rotational inertia, angle of approach, etc…). In addition, both methods will provide a step by step graphical representation to assure a solid approach to physical fundamentals. Conclusions will be presented when the results to a similar scenario can be compared.

Nomenclature

M	Mass of vehicle
I	Moment of inertia of vehicle
k	Radius of gyration of vehicle
Ψ	Angular acceleration of vehicle
h	Moment arm of the force acting through P
P	Centroid of crush and common velocity point
ΔV	Change in velocity for vehicle at CG
ΔV_{ω}	Change in velocity for vehicle due to inertial mass
ΔV_P	Change in velocity for vehicle at point P
R	Resitive element
0	0 junction
f	Effort variable representing a force
T	Effort variable representing a torque
v	Flow variable representing a velocity
ω	Flow variable representing an angular velocity
TF	Transformer ratio
M_{eq}	Equivalent mass of vehicle
M_{eff}	Effective mass of system
v_{cP}	Closing velocity of point P
x_{cP}	Closing distance of point P
E_R	Net energy absorbed by R
ε	Coefficient of restitution
$v_{cP\ before}$	Closing velocity of point P before impact
$v_{cP\ after}$	Closing velocity of point P after impact
γ	Non-dimensional term relating the properties of the CG to the point P

I	Impulse of system
P	Power flowing through a branch
$\overline{M}$	Non-dimensional mass of vehicle
$\overline{M}_{\omega}$	Non-dimensional inertial mass of vehicle
$\overline{M}_{eq}$	Non-dimensional equivalent mass of vehicle
$\overline{M}_{eff}$	Non-dimensional effective mass of system
$\overline{h}$	Non-dimensional moment arm of the force acting through P
$\overline{I}$	Non-dimensional impulse of system
$\overline{E}_R$	Non-dimensional net energy dissipated
$\overline{\Delta V}$	Non-dimensional change in velocity for vehicle at CG
$\overline{\Delta V}_{\omega}$	Non-dimensional change in velocity for vehicle due to inertial mass
$\overline{\Delta V}_{p}$	Non-dimensional change in velocity for vehicle at point P
$\overline{\Delta E}_{p}$	Non-dimensional impulse in power
$\overline{v}_{cP\,before}$	Non-dimensional closing velocity of point P before impact
$\overline{v}_{cP\,after}$	Non-dimensional closing velocity of point P after impact
$\overline{\Delta E}$	Non-dimensional impulse in power for the translational system
$\overline{\Delta E}_{\omega}$	Non-dimensional impulse in power for the rotation system
$\widetilde{v}_{cP}$	Average velocity corresponding to the power impulse during the impact
θ_1	Angle relating n-t axes from x-y axes
x , y	Coordinate of P defined relative to the CG of vehicle
n , t	Moment arm for impulses from point P to the CG of vehicle
W_L	Width of the vehicle
a	Length from CG to the front bumper of vehicle
b	Length from CG to the back bumper of vehicle
θ	Angle at which vehicle 2 is approaching vehicle 1
v	Translational velocity of vehicles prior to impact
ω	Rotational velocity of vehicle prior to impact
μ	Impulse ratio
μ_o	Critical impulse ratio
V_x	Translational velocity of vehicle after impact in x direction
V_y	Translational velocity of vehicle after impact in y direction
Ω	Rotational velocity of vehicle after impact.
CV_x	Closing velocity of vehicle before impact in x direction
CV_y	Closing velocity of vehicle before impact in y direction
$PDOF$	Principal direction of force
c_i	Crush depth measurement from origin of crush
w_i	Width measurements from origin of crush
C	Crush matrix
W	Width matrix
P_x	Width coordinate for the point P from origin of crush
P_y	Depth coordinate for the point P from origin of crush

E	Energy absorbed in plastic deformation
$E1$	Adjusted energy calculation of vehicle 1 as a function of θ_E
A	Spring preload coefficient
B	Spring constant per unit width coefficient
F	Estimated force through point P
θ_E	Estimated direction of the force through the point P of vehicle 1
θ_2	Estimated direction of the force through the point P of vehicle 2
$E2$	Adjusted energy calculation of vehicle 2 as a function of θ_2
d	Distance from point P to CG of vehicle
$V_{separation_x}$	Separating velocity of vehicle after impact in x direction
$V_{separation_y}$	Separating velocity of vehicle after impact in y direction
θCV	Value of closing velocity for a given θ_E
$\theta V_{separation}$	Value of separating velocity for a given θ_E
$\theta \Delta V$	Value of change in velocity for a given θ_E
θv	Value of velocity before impact for a given θ_E
θV	Value of velocity after impact for a given θ_E

CHAPTER 2: ANALYTICAL MODEL OF THE SYSTEM

Objective

The approach used in CRASH3 to develop a single, closed-form damage analysis technique that could be applicable to collision configuration is derived for the case of central collisions, (where the line of action of the collision passes through the centers of masses of the two vehicles) and a more general case of non central collision [17]. For either case, the two vehicles are modeled as a spring-mass system where the springs represent the linear peripheral crush of the area of contact for each car. The velocity changes experienced by vehicle 1 and 2 during the approach period of the collision are obtained from the solution to the simple differential equation of the form:

$$m\ddot{x} + k\,x = 0 \tag{2.1}$$

The objective of this chapter is to show that the same closed form solution can be obtained using an approach that does not require the representation of a linear spring (crush of the car modeled as a linear spring) and does not assume simple harmonic motion as a trivial solution. Terms pertinent to the new approach will be defined and it will be shown how the energy transferred during the impact phase can be modeled as power impulses applied to each vehicle element, with a single force impulse for any given collision.

The Model

A collision can be described as a brief event in which two or more bodies come together resulting in an exchange of energy and momentum, including a change of direction. In automobile reconstruction, a collision can either be central or non-central. A collision is defined central when the line of action of the collision force passes through the centers of the masses of the two vehicles [17]. In non-central collisions, a common velocity is achieved at the region of collision contact rather than at the center of gravity [17]. The non-central frontal collision depicted in Figure 2-1 will be used to obtain a solution for the velocity changes experienced by Vehicles 1 and 2. In Figure 2-1 a common velocity is reached at point *P* although the model can include relative velocities between points *P* on each vehicle.

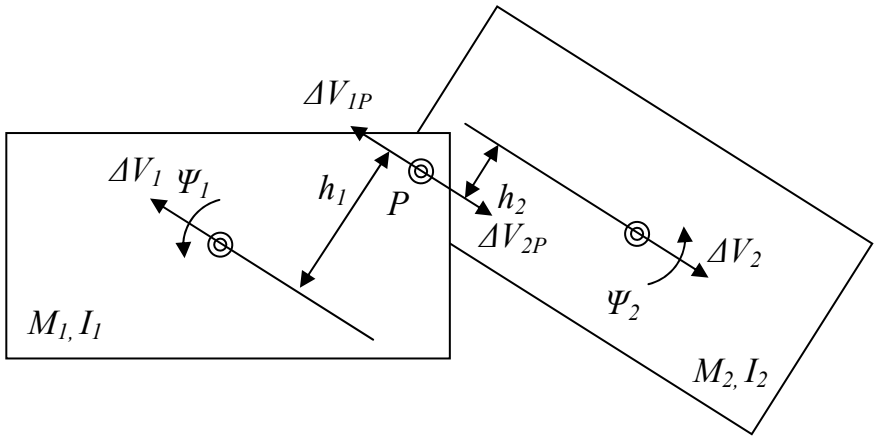

Figure 2-1: Non-central frontal collision

Figure 2-2 illustrates the modeling of Figure 2-1 using a bond graph approach. Let the energy dissipated during the impact phase due to the crushing of the cars be

modeled as a resistive type element acting at point P. Let the power flow from the resistive type element into a 0 junction. In order to relate the power flow from the point *P* to the center of gravity of each vehicle, two other 0 junctions are created. The inertial elements are represented through a transformer and in parallel with their corresponding mass. Because inertia effects are analogous to masses, the equivalent inertial mass seen by the system is the product of the transformer ratio with the mass of the system. The transformer does not create, store, or destroy energy. It conserves power and transmits the factors of power with proper scaling as defined by the transformer ratio. This transformer ratio is the moment arm described by Expression 2.2 for vehicle 1and Expression 2.3 for vehicle 2.

$$h_1 \tag{2.2}$$

$$h_2 \tag{2.3}$$

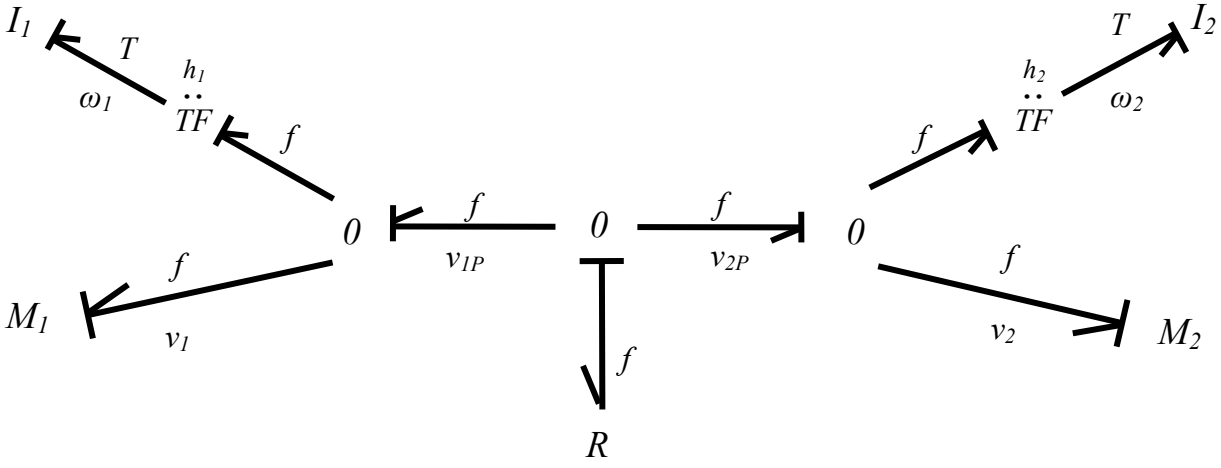

Figure 2-2: Non-central collision modeling

Consider the 0 junction illustrated in Figure 2-3. 0 junctions are governed by the following rules. The effort variable must be equal on each branch while the algebraic

sum of the flow variables is zero. In a mechanical system, the effort variable represents either a force or torque acting on the system while the flow variable represents the velocity or the angular velocity corresponding to its effort variable. Figure 2.3 reduces to the identity presented in Figure 2-4.

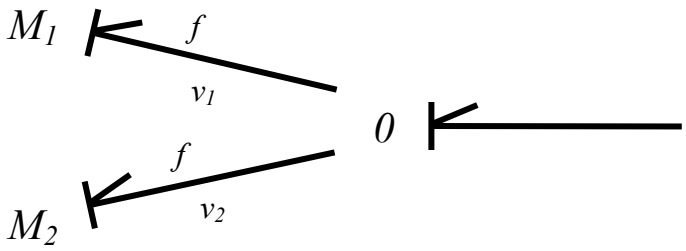

Figure 2-3: A 0 junction

This is acceptable since the inverse of the equivalent mass of two objects in parallel is equal to the sum of their inverse. In other words, $\frac{1}{M_{eq}} = \frac{1}{M_1} + \frac{1}{M_2}$ or

$$M_{eq} = \frac{M_1 M_2}{M_1 + M_2} \tag{2.4}$$

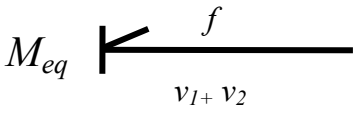

Figure 2-4: Identity 0 junction

The equivalent inertial mass of vehicle 1 seen by the system is represented in Figure 2-5.

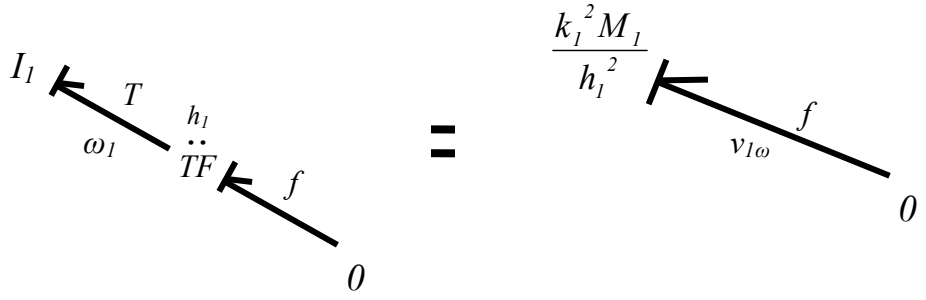

Figure 2-5: Equivalent inertial mass of vehicle 1

Notice that the flow variable is also transformed and represents the velocity relative to the velocity of the centroid of the vehicle at point *P* corresponding to rotation of each vehicle. If we apply the identity proposed in Figure 2-3 and Figure 2-4 to each of the side 0 junctions of Figure 2-2, the model simplifies to one 0 junction and 2 equivalents masses. The equivalent mass for each vehicle can be determined from Equation 2.4 as follows.

$$M1_{eq} = \frac{M_1 \frac{k_1^2 M_1}{h_1^2}}{M_1 + \frac{k_1^2 M_1}{h_1^2}} \Rightarrow M_1 \frac{k_1^2}{k_1^2 + h_1^2} \tag{2.5}$$

In a similar manner for vehicle 2,

$$M2_{eq} = M_2 \frac{k_2^2}{k_2^2 + h_2^2} \tag{2.6}$$

Figure 2-2 transforms into Figure 2-6. Notice that the identity proposed in Figures 2-3 and 2-4 has also been applied to the equivalent system of both masses to reduce the system to one effective mass M_{eff}.

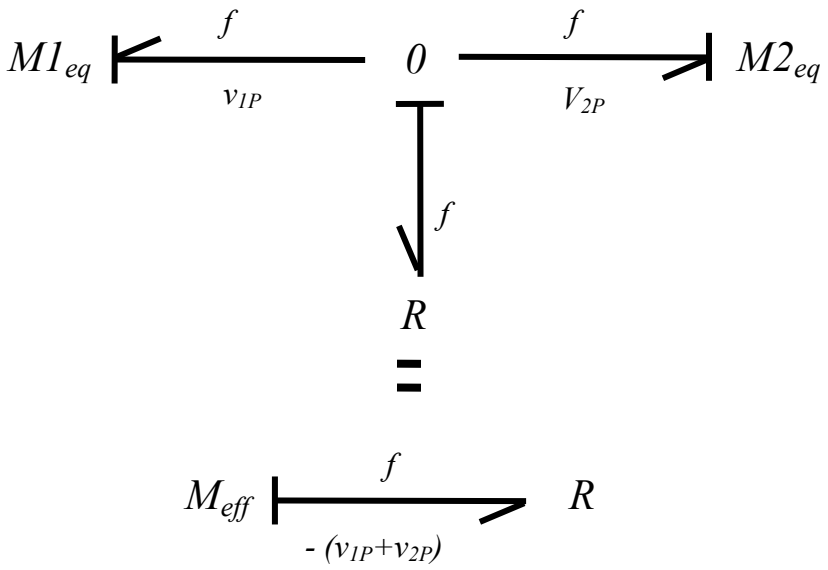

Figure 2-6: Effective mass of the system

The effective mass of the system is defined as:

$$M_{eff} = \frac{\left(M_1 \frac{k_1^{\,2}}{k_1^{\,2} + h_1^{\,2}}\right)\left(M_2 \frac{k_2^{\,2}}{k_2^{\,2} + h_2^{\,2}}\right)}{\left(M_1 \frac{k_1^{\,2}}{k_1^{\,2} + h_1^{\,2}}\right) + \left(M_2 \frac{k_2^{\,2}}{k_2^{\,2} + h_2^{\,2}}\right)} \tag{2.7}$$

The energy dissipated during a collision between vehicle 1 and vehicle 2 is analogous to the energy dissipated by one vehicle of mass M_{eff} into a rigid barrier. The constitutive equation for the mass element of a mechanical system relates the momentum to the flow variable. Stated differently, $v = \frac{1}{M}\int f\,dt$ or $f = M\frac{dv}{dt}$. Applying Newton's second law to the effective system of Figure 2-6 yields Equation 2.8.

$$-f = M_{eff}\frac{dv_{cP}}{dt} \tag{2.8}$$

where $v_{cP} = -(v_{1P} + v_{2P})$. When we algebraically multiply v_{cP} on both side of Equation 2.8, the left hand side of Equation 2.9 becomes the power flowing through the bond on the left of the equation while the right hand section is the power flowing into the effective mass, M_{eff}:

$$-f\, v_{cP} = M_{eff} \frac{dv_{cP}}{dt} v_{cP} \tag{2.9}$$

If we modify v_{cP} to be the rate of change of x_{cP}, Equation 2.10 is created.

$$M_{eff} \frac{dv_{cP}}{dt} v_{cP} = -f \frac{dx_{cP}}{dt} \Rightarrow M_{eff} dv_{cP} v_{cP} = -f\, dx_{cP} \tag{2.10}$$

Integrating both sides of Equation 2.10 yields the following critical equation:

$$\frac{1}{2} M_{eff} \left(v_{cP\,after}{}^2 - v_{cP\,before}{}^2 \right) = -E_R \tag{2.11}$$

Notice that E_R is nothing more than the net energy absorbed by the resistive type element and its value is valid for any force vs. displacement curve, linear or not. If we wanted to account for restitution, Equation 2.11 would simplify to:

$$v_{cP\,before}{}^2 \left(1 - \varepsilon^2\right) = \frac{2E_R}{M_{eff}} \tag{2.12}$$

where $\varepsilon = \left| \frac{v_{cP\,after}}{v_{cP\,before}} \right|$

Note that the " resistive" element stores some energy which is returned during spring back and thus acts as a combination spring and dissipative element. ε is often seen in the literature as a restitution coefficient. In our model, the coefficient of restitution acts in the direction of the force. $v_{cP\,before}$ represents the closing velocity of point *P* of vehicle1 and vehicle2 which is their velocity difference before impact.

Consider h_1, the moment arm of the force acting through *P* for vehicle 1. The corresponding moment acting on vehicle 1 is:

$$F_x h_1 = -I_1 \ddot{\psi}_1 = -M_1 k_1^2 \ddot{\psi}_1 \tag{2.13}$$

where $\ddot{\psi}_1$ is the angular acceleration and k_1 is the radius of gyration of vehicle 1. The changes in velocity for each vehicle at their respective point *P* can be determined from Equation 2.12. Equations 2.14 and 2.15 illustrate that relationship for each vehicle. For vehicle 1,

$$\Delta V_{1P} = \sqrt{\frac{2(E_R)}{M_{eff}(1-\varepsilon^2)}} \frac{M2_{eq}}{M2_{eq} + M1_{eq}}(1+\varepsilon) \tag{2.14}$$

And for vehicle 2,

$$\Delta V_{2P} = \sqrt{\frac{2(E_R)}{M_{eff}(1-\varepsilon^2)}} \frac{M1_{eq}}{M2_{eq} + M1_{eq}}(1+\varepsilon) \tag{2.15}$$

As shown in Equations 2.5 and 2.6, the non-dimensional terms, γ_1 and γ_2 relating the properties of the center of gravity to the point P, is defined such that:

$$\Delta V_1 = \gamma_1 \Delta V_{1P}. \tag{2.16}$$

where $\gamma_1 = \frac{k_1^2}{k_1^2 + h_1^2}$ and $\gamma_2 = \frac{k_2^2}{k_2^2 + h_2^2}$

It should be noted that when $\gamma_1 = \gamma_2 = 1$, the general solution to the non-central collision reduces to a central collision. When $\varepsilon = 0$, the solution given in CRASH3 is identical to Equation 2.16.

Impulse in Power

Initially, we will define the force impulse of the system. Multiplication of the derivative in time and integrating both sides of Equation 2.8 with respect to time helps us to recognize that the force impulse of the system (Figure 2-6) is the change in momentum of the system.

$$-fdt = M_{eff}\,dv_{cP} \Rightarrow \int -fdt = \int M_{eff}\,dv_{cP} \Rightarrow -I = M_{eff}\left(v_{cP\,after} - v_{cP\,before}\right) \qquad (2.17)$$

Also expressed in terms of the velocity change of car1, $I_1 = \gamma_1 M_1\,\Delta V_{1P}$ or $I_1 = M1_{eq}\,\Delta V_1$. The impulse of the system is conserved, therefore $I = I_1 = I_2$. Relating Equation 2.9 to one of the equivalent mass system yields:

$$-f = M1_{eq}\frac{dv_{cP1}}{dt} \qquad (2.18)$$

When we algebraically multiply v_{cP1} on both sides of Equation 2.18, the left hand side becomes power and represents the power flow into the mass $M1_{eq}$

$$-f\,v_{cP1} = M1_{eq}\frac{dv_{cP1}}{dt}v_{cP1} = P_1 \qquad (2.19)$$

Similarly, for the second equivalent mass system,

$$-f\,v_{cP2} = M2_{eq}\frac{dv_{cP2}}{dt}v_{cP2} = P_2 \qquad (2.20)$$

The 0 junction in Figure 2-6 tells us that power flowing out of R equals the summation of the power flowing into the equivalent masses such that:

$$M1_{eq}\frac{dv_{cP1}}{dt}v_{cP1} + M2_{eq}\frac{dv_{cP2}}{dt}v_{cP2} = P_1 + P_2 = -P_3 \qquad (2.21)$$

The integral of the power with respect to the derivative in time is energy. Algebraically Equation 2.21 can be reduced to:

$$M1_{eq}\, dv_{cP1} v_{cP1} + M2_{eq}\, dv_{cP2} v_{cP2} = -P_3 dt \tag{2.22}$$

The right hand side of Equation 2.22 when integrated becomes what is referred in this work as an impulse in power. It also represents the energy dissipated during the impact phase due to the crushing of the vehicles. Integrating both sides of Equation 2.22 gives us the following identity:

$$\frac{1}{2} M1_{eq} \left(v_{cP1\,before}{}^{2} - v_{cP1\,after}{}^{2} \right) + \frac{1}{2} M2_{eq} \left(v_{cP2\,before}{}^{2} - v_{cP2\,after}{}^{2} \right) = E_R \tag{2.23}$$

Figures 2-2 and 2-5 shows that the velocity at point *P* for vehicle one is the sum of a "translational velocity" v_1 and a "rotational velocity" $v_{1\omega}$. Therefore,

$$\Delta V_{1P} = \Delta V_1 + \Delta V_{1\omega} \tag{2.24}$$

To satisfy Equation 2.24, $\Delta V_{1\omega} = \left(1 - \gamma_1\right) \Delta V_{1P}$, since $\Delta V_1 = \gamma_1\, \Delta V_{1P}$. This allows us to further quantify energy as it flows through each branch of the bond graph. From Equation 2.23, it is evident that if the change in energy dissipated by the resistive type element is known, the change in energy for both equivalent masses can be determined under one condition. This condition will be addressed in Chapter 3.

CHAPTER 3: NON-DIMENSIONAL MODEL OF THE SYSTEM

Objective

In Chapter 2, we used the bond-graph approach to represent a two dimensional planar impact collision between two vehicles. From our model, we were able to derive the solution to the velocity changes experienced by vehicle 1 and vehicle 2 during the impact period of the collision. We showed that the solution obtained is identical to the solution developed in CRASH3. The objective of this chapter is to establish a consistent sign convention that relates the physical phenomena to the modeled system. In addition, we will non-dimensionalize the equations found in Chapter 2 and define all of the changes in energy as a function of a characteristic velocity. Finally, we will derive an expression for the average velocity experienced by each vehicle during impact as a function of their power impulse.

Momentum Exchange

The bond-graph represented in Figure 2-2 is valid for both the pre-impact and the post-impact stages of the collision. From conservation of momentum, we can relate the ratio of each mass to the ratio of their change in velocity as displayed in Equation 3.1.

$$\frac{M_1}{M_2} = \frac{\Delta V_2}{\Delta V_1} \tag{3.1}$$

As seen in Chapter 2, Equation 2.12 was the critical equation that was used to determine the change in velocity of the each vehicle. Each branch of the system has an equivalent

force, therefore during impact all effective masses see the same force impulse called the impulse of the system. The impulse of the system is defined from Equations 2.12 and 2.17 and can be rewritten as:

$$I = M_{eff}\left(1+\varepsilon\right)\sqrt{\frac{2E_R}{M_{eff}\left(1-\varepsilon^2\right)}} \tag{3.2}$$

The characteristic variables for the system are chosen as mass of vehicle 1 for the characteristic mass, the radius of gyration of vehicle 1 for the characteristic distance and the closing velocity of the system in the direction of the force as a substitute for the characteristic time. A non dimensional variable is a variable divided by its characteristic variable. In non dimensional From, $\overline{M}_1$ becomes:

$$\frac{M_1}{M_1} = 1 \tag{3.3}$$

In a similar way, $\overline{M}_2 = \frac{M_2}{M_1}$. Recall, the equivalent inertial mass $M_{1\omega} = \frac{k_1^{\,2}}{h_1^{\,2}} M_1$, its non dimensional form is,

$$\overline{M}_{1\omega} = \frac{k_1^{\,2}}{h_1^{\,2}} \Rightarrow \frac{1}{\bar{h}_1} \tag{3.4}$$

In a similar way, $\overline{M}_{2\omega} = \frac{1}{\bar{h}_2}\ \overline{M}_2$, $\overline{M1}_{eq} = \frac{1}{1+\bar{h}_1}$, $\overline{M2}_{eq} = \frac{\overline{M}_2}{1+\bar{h}_2}$, and

$$\overline{M}_{eff} = \frac{\overline{M}_2}{\bar{h}_1\overline{M}_2 + \bar{h}_2 + \overline{M}_2 + 1}.$$

where $\bar{h}_1 = \frac{h_1^{\,2}}{k_1^{\,2}}$ and $\bar{h}_2 = \frac{h_2^{\,2}}{k_2^{\,2}}$.

Equation 2.2 can also be written in a non-dimensional form as shown in Equation 3.5.

$$\bar{I} = \overline{M}_{eff}\left(1+\varepsilon\right)\sqrt{\frac{2\bar{E}_R}{\overline{M}_{eff}\left(1-\varepsilon^2\right)}} \tag{3.5}$$

where $\bar{E}_R = \dfrac{2E_R}{M_1 v_{cP\,before}{}^2}$

$\bar{E}_R$ is the non-dimensional form of the energy dissipated during impact as seen in Equation 2.23. It also represents the ratio of the total actual crush energy to the crush energy that would be caused by vehicle 1 impacting a fixed barrier at the closing velocity of both vehicles. From Figure 2-2, the non dimensional change of velocity at point *P* for vehicle 1 is

$$\overline{\Delta V}_{1p} = \bar{I}\left(1+\bar{h}_1\right) \tag{3.6}$$

Notice that the expression defined in Equation 3.6 has a different form than that of Equation 2.14 but their values would be identical if Equation 2.14 were non-dimensionalized (shown below). The other 5 non-dimensional changes of velocity are described as follows:

$$\overline{\Delta V}_{2p} = \frac{\bar{I}\left(1+\bar{h}_2\right)}{\overline{M}_2},\quad \overline{\Delta V}_1 = \bar{I},\quad \overline{\Delta V}_{1\omega} = \bar{I}\bar{h}_1,\quad \overline{\Delta V}_2 = \frac{\bar{I}}{\overline{M}_2},\quad \overline{\Delta V}_{2\omega} = \frac{\bar{I}\bar{h}_2}{\overline{M}_2}.$$

These expressions are valid and are only dependant upon the following primary variables: the masses, the radii of gyration, the moment arms from the direction of the force to the center of gravity and the total energy dissipated during the impact. As mentioned above, Equation 2.14 is identical to Equation 3.6 but represented in a different form. In non-dimensional form, Equation 2.14 becomes

$$\overline{\Delta V}_{1P} = \frac{\overline{M}_2\left(1+\bar{h}_1\right)}{\overline{M}_2\bar{h}_1 + \bar{h}_2 + \overline{M}_2 + 1}\left(1+\varepsilon\right) \tag{3.7}$$

Equation 3.7 is much more descriptive of the system. In other words, all of the non dimensional changes in velocity for all branches of any system can be determined from four ratios. These four ratios are $\overline{M}_2$, $\bar{h}_1$, $\bar{h}_2$, and ε. In addition, the dimensional forms of those changes in velocity can be determined as long as E_R and M_1 for that system is known. Rewritten in the more descriptive form, Equation 3.7 becomes

$$\overline{\Delta V}_{1P} = \frac{\overline{M}_2 \gamma_2}{\left(\overline{M}_2 \gamma_2\right) + \gamma_1}\left(1+\varepsilon\right) \tag{3.8}$$

where $\gamma_1 = \frac{1}{1+\bar{h}_1}$ and $\gamma_2 = \frac{1}{1+\bar{h}_2}$.

Similarly, the other 5 non-dimensional changes of velocity are described as follows:

$$\overline{\Delta V}_{2P} = \frac{\gamma_1}{\gamma_1 + \left(\overline{M}_2 \gamma_2\right)}\left(1+\varepsilon\right), \qquad \overline{\Delta V}_1 = \overline{\Delta V}_{1P}\gamma_1, \qquad \overline{\Delta V}_{1\omega} = \overline{\Delta V}_{1P}\left(1-\gamma_1\right),$$

$$\overline{\Delta V}_2 = \overline{\Delta V}_{2P}\gamma_2, \qquad \overline{\Delta V}_{2\omega} = \overline{\Delta V}_{2P}\left(1-\gamma_2\right).$$

Energy Exchange

The impulse in power or power impulse represented by Equation 3.2 can also be interpreted as the change in energy experienced by the equivalent system. As shown in Equation 2.23, this energy exchange is not directly proportional to the change in velocity but rather the change of the individual pre and post velocity squared. Therefore, only knowing the change in velocities is not enough to ascertain the portion of energy change for each bond. It is important to clarify the possibility for confusion. The change in energy for one vehicle going from 20 mph to 10 mph will be greater than the change in energy for the same vehicle going from 15 mph to 5 mph even though they have similar

changes in velocity. Equation 2.23 compartmentalizes the impulses in power for the central 0 junction of Figure 2-2. The non-dimensional impulse in power for the equivalent system of vehicle 1 can be reduced to Equation 3.9.

$$\overline{\Delta E}_{1p} = \frac{1}{2}\overline{M1}_{eq}\left(\left(\bar{v}_{cP1\,before}\right)^2 - \left(\bar{v}_{cP1\,after}\right)^2\right) \tag{3.9}$$

Let us assume that the velocity before impact at point *P* on vehicle 1 is given the value of the characteristic velocity. Therefore,

$$\bar{v}_{cP1\,before} = 1 \tag{3.10}$$

and using Equation 2.6, the velocity after impact at point *P* is calculated as follows:

$$\bar{v}_{cP1\,after} = \overline{\Delta V}_{1p} + \bar{v}_{cP1\,before} \tag{3.11}$$

Equations 3.10 and 3.11 can be substituted back into 3.9. As far as the non-dimensional impulse in power for the equivalent system of vehicle 2, two approaches leading to identical results can be used. The first one satisfies Equation 2.23 as follow

$$\overline{\Delta E}_{2p} = \overline{E}_R - \overline{\Delta E}_{1p} \tag{3.12}$$

The second approach uses Figure 2-6 to evaluate the value of v_{p2} from the following identity $v_{cP} = -\left(v_{p1} + v_{p2}\right)$. In non-dimensional form,

$$\bar{v}_{cP2\,before} = -\sqrt{\frac{2\overline{E}_R}{\overline{M}_{eff}\left(1-\varepsilon^2\right)}} - \bar{v}_{cP1\,before} \tag{3.13}$$

Similar to Equations 3.9 and 3.11, Equations 3.14 and 3.15 are formulated as follow:

$$\bar{v}_{cP2\,after} = \overline{\Delta V}_{2p} + \bar{v}_{cP2\,before} \tag{3.14}$$

$$\overline{\Delta E}_{2p} = \frac{1}{2}\overline{M2}_{eq}\left(\left(\bar{v}_{cP2\,before}\right)^2 - \left(\bar{v}_{cP2\,after}\right)^2\right) \tag{3.15}$$

Using the same approach for the other two 0 junctions allows us to further quantify the change in energy into the translational and the rotational equivalent systems. In the special case where vehicle 1 has no initial rotational velocity, the velocity before impact of the center of gravity of vehicle 1 is also given the value of the characteristic velocity since $v_{1P} = v_1 + v_{1\omega}$. The non-dimensional impulse in power for the translational system is given as:

$$\overline{\Delta E}_1 = \frac{1}{2}\overline{M}_1\left(\left(\bar{v}_{cP1\,before}\right)^2 - \left(\overline{\Delta V}_1 + \bar{v}_{cP1\,before}\right)^2\right) \tag{3.16}$$

and the non-dimensional impulse in power for the rotational system of vehicle 1 is:

$$\overline{\Delta E}_{1\omega} = \frac{1}{2}\overline{M}_{1\omega}\left((0)^2 - \left(\overline{\Delta V}_{1\omega} + 0\right)^2\right) \tag{3.17}$$

Under similar assumption for vehicle 2, the non-dimensional impulse in power for the translational system is given as:

$$\overline{\Delta E}_2 = \frac{1}{2}\overline{M}_2\left(\left(\bar{v}_{cP2\,before}\right)^2 - \left(\overline{\Delta V}_2 + \bar{v}_{cP2\,before}\right)^2\right) \tag{3.18}$$

and the non-dimensional impulse in power for the rotational system of vehicle 2 is:

$$\overline{\Delta E}_{2\omega} = \frac{1}{2}\overline{M}_{2\omega}\left((0)^2 - \left(\overline{\Delta V}_{2\omega} + 0\right)^2\right) \tag{3.19}$$

It is beneficial to plot the changes in energy of each branch and see how they vary as a function of the velocity of vehicle 1 prior to impact. If vehicle 1 has an initial velocity of value negative two times the closing velocity, vehicle 2 will be imposed an initial velocity of one times the closing velocity in order to maintain a closing velocity of 1. Let the abscissa of the plot representing the initial velocity of vehicle 1 vary from -2 to 1. Figure 3-1 is a graphical representation of the plots assuming that both vehicles are

identical, $M_1 = M_2 = 3500\ lb$, both radii of gyration and moment arms are identical $k_1 = k_2 = h_1 = h_2 = 4\ ft$ and $E_R = 10{,}000\ lbf\text{-}ft$.

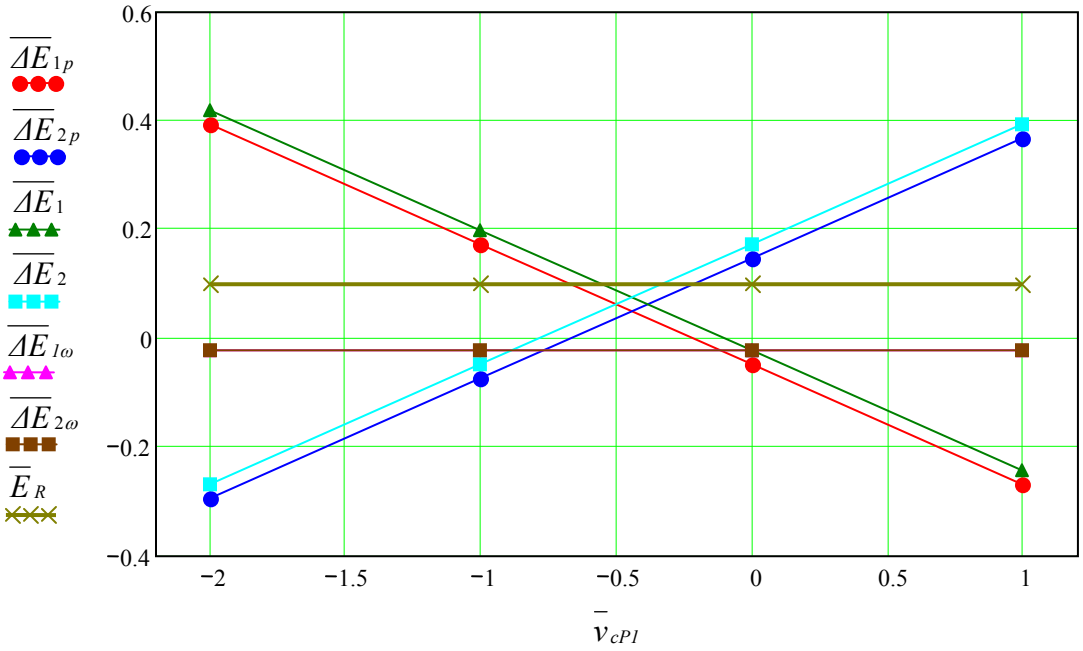

Figure 3-1: Plot of the non-dimensional energy changes vs. initial velocity of vehicle 1

A positive change in energy means a loss or a discharge of energy and a negative value represents a gain or absorbing energy. The changes of energy vary linearly as a function of the initial velocity of vehicle 1. This is explained by Equation 3.20. Rewriting Equation 3.7 in a different form with the change in velocity known gives:

$$\overline{\Delta E}_{1p} = \frac{1}{2}\overline{M1}_{eq}\left(\left(\overline{\Delta V}_{1p}\right)^2 + \left(2\overline{\Delta V}_{1p}\bar{v}_{cP1before}\right)\right) \tag{3.20}$$

We showed earlier in Equation 2.21 that the power impulse was a function of the force times a velocity. Integrating both sides allows us to define a new term $\tilde{v}_{cP2}$.

$$\int P_2 dt = \int f\, v_{cP2} dt \Rightarrow \widetilde{v}_{cP2} \int f\, dt \Rightarrow \widetilde{v}_{cP2} I \tag{3.21}$$

$\widetilde{v}_{cP2}$ is the average velocity of the branch corresponding to the power impulse during the impact. In non-dimensional form,

$$\widetilde{v}_{ci} = \frac{\overline{\Delta E_i}}{\bar{I}} \quad \text{with} \quad \text{i} = 1..6 \text{ branches} \tag{3.22}$$

A similar plot to Figure 3-1 can be assembled. However it is the same plot simply scaled by $\frac{1}{\bar{I}}$.

CHAPTER 4: ENERGY APPROACH USING MATHCAD

Objective

As mentioned in the literature review of Chapter 1, one of the approaches to reconstructing accidents is the momentum based approach, elaborated in a general form by Brachs in their book "Vehicle Accident Analysis and Reconstruction Methods" [4]. This traditional approach uses a set of equations to calculate the velocity components of two colliding vehicles after impact. The objective of this chapter is to demonstrate that the energy method used by CRASH3 uses the same fundamental physical principles as the momentum approach and that for any given accident scenario, both methods provide identical results. Because the approach to both methods is different, the input requirements are also different. The work will be presented in the form of MathCAD work sheets that will allow the user to reconstruct a wide variety of accidents while controlling just a few parameters (i.e. mass, rotational inertia, angle of approach, etc…). In addition, these modules will provide a set of graphical representations in order to facilitate the physical interpretation of the scenario. In the case when there is no restitution and no sliding, we will extend the solution provided in CRASH3 by calculating the velocity prior to and after impact for both vehicles. We will also show how the direction of the force between two vehicles can be determined from the ratio of their velocities prior to impact.

The Momentum Module

The purpose of this module is to provide a set of solutions for a given scenario. Because the set of equations for the momentum approach are very well defined in Brach's book [4], we will not show how these equations are derived. However, we will show how they are used in a modular form and how the graphical representation can be compared to the energy module that will be discussed hereafter. The required input for the momentum method can be categorized as follows: the initial velocity components (translational and rotational), the physical properties of the vehicles (masses and rotational inertias), the orientation angles (headings) and the collision-damage characteristics (point of contact, orientation of n-t axes, restitution coefficient, impulse ratio).

In order to simplify calculations, we assume that vehicle 1 is always heading in the y direction. The center of gravity (CG) of each vehicle is located at the origin. For graphical representation, each vehicle is defined by three parameters. These parameters are: the width of the vehicle, the length from CG to the front bumper and to the back bumper. It is important to mention that changing these variables from one scenario to another will not affect the results but are used only for graphical description. The point of contact *P* is defined relative to the CG of each vehicle using an x and y components referred to as x_1 and y_1 as shown in Figure 4-1. The angle relating the normal and tangential coordinate system set (n-t axes) from the fixed coordinate system (x-y axes) is specified by θ_1. If θ_1 is 0 degrees, the moment arm for each impulse component from point *P* to the CG is x_1 and y_1. Otherwise, their values have to be adjusted as θ_1 changes by the following expressions:

$$n_1 = x_1 \sin(\theta_1) - y_1 \cos(\theta_1) \tag{4.1}$$

$$t_1 = x_1 \cos(\theta_1) - y_1 \sin(\theta_1) \tag{4.2}$$

From Figure 4-1, see how the moment arms for each impulse component graphically changes as θ_1 changes.

In our module, vehicle 2 is always making contact with vehicle 1. Whether the collision is a central impact or a non-central impact, the angle θ represents the angle at which vehicle 2 is approaching vehicle 1. Specifying a value for θ is identical to assuming a specific direction for the velocity of vehicle 2 before impact. The values for θ_1 or θ are not always known accurately prior to the collision and therefore can be

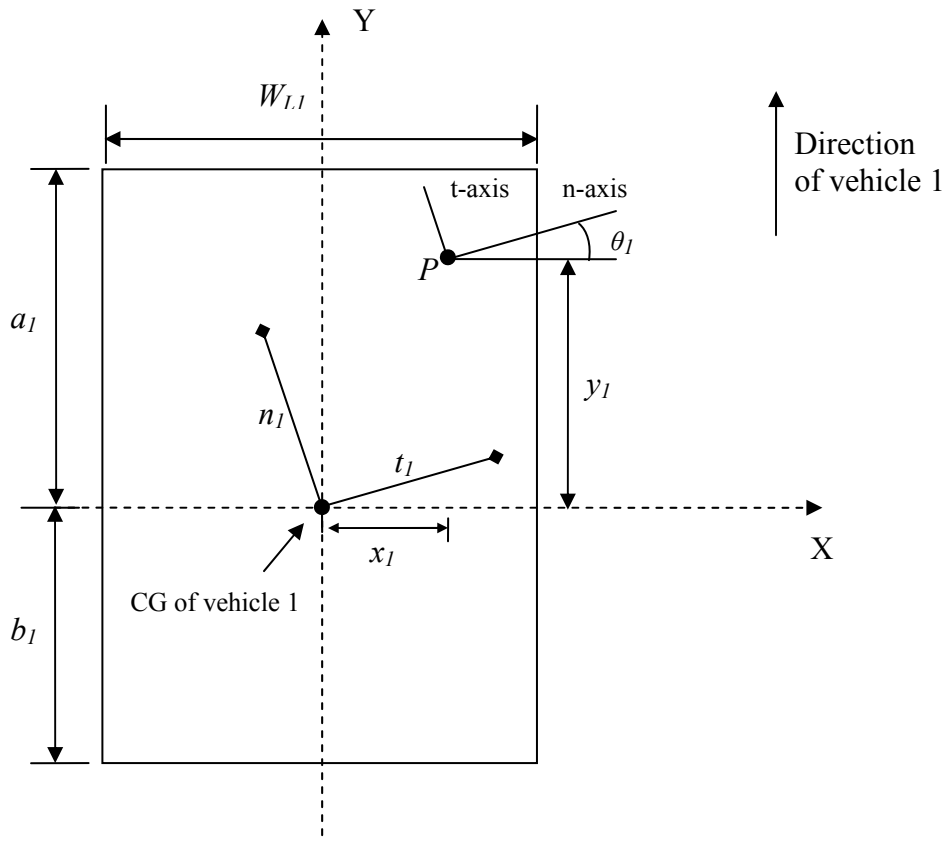

Figure 4-1 Graphical representation of vehicle 1

changed independently to optimize the results. θ is assumed positive counter clockwise and negative clockwise. Figure 4-2 is a graphical representation of vehicle 2 contacting vehicle 1 at an angle θ. Notice that θ_1 remains unchanged because it is a common variable to the reference coordinate system (x-y).

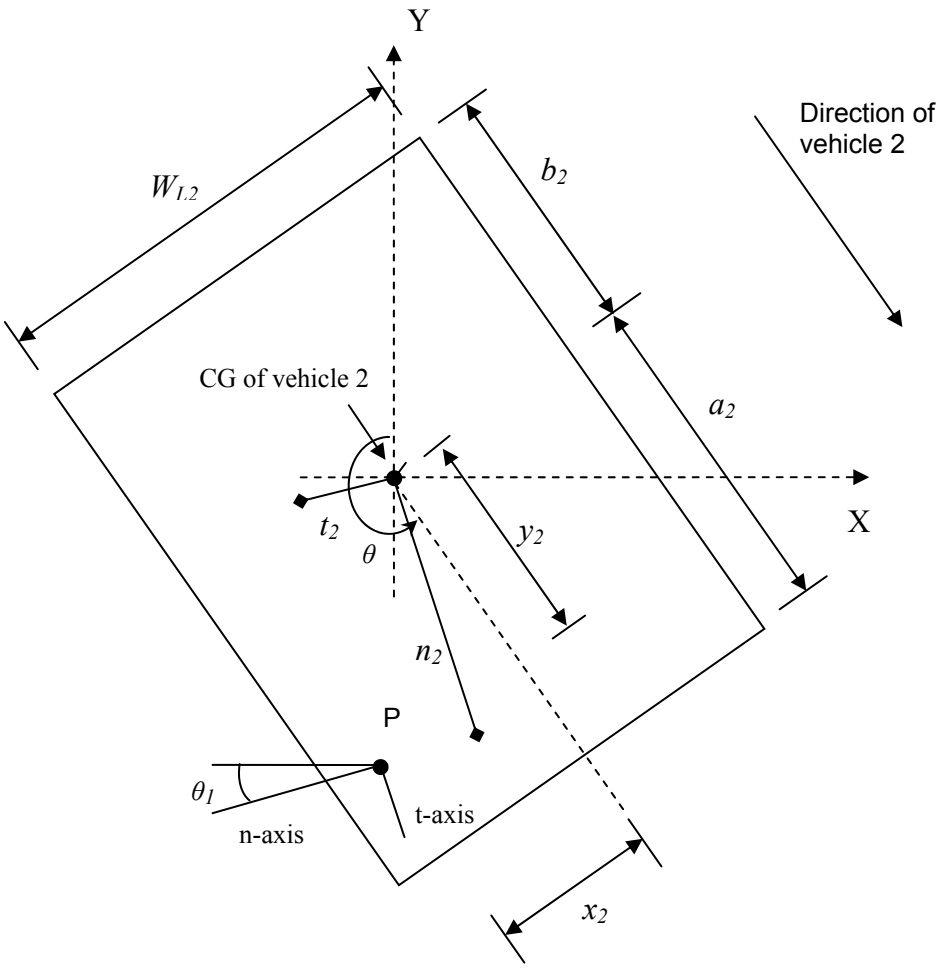

Figure 4-2 Graphical representation of vehicle 2

Similarly to vehicle 1, the moment arms for each impulse component for vehicle 2 can be graphically represented as shown in Figure 4-2. Their directions and magnitudes can be calculated from Equations 4.3 and 4.4.

$$n_2 = x_2\ sin(\theta_2) - y_2\ cos(\theta_2) \tag{4.3}$$

$$t_2 = x_2\ cos(\theta_2) - y_2\ sin(\theta_2) \tag{4.4}$$

With $\theta_2 = -[\pi - [\theta_1 + (2\pi - \theta)]]$

Now that the graphical representation of the module has been introduced, we will analyze the specific scenario depicted by table 1.

Table 4-1: Input for momentum module

	Vehicle 1	Vehicle 2
M (lb)	4000	3500
k (ft)	4.484	4.288
a (in)	80	80
b (in)	60	60
W_L (in)	80	80
θ (deg)	0	-150
x (in)	24	24
y (in)	60	60
v (mph)	20	40
ω (deg per sec)	0	0

θ_1 (deg)	ε	μ
6.141	0	100% μ_0

The lower case v represents the translational velocity of both vehicles prior to impact but their value only indicates their magnitude. The relative direction in which they are going is represented by θ. The lower case ω represents the rotational velocity of both vehicles

prior to impact. The symbol ε represents the coefficient of restitution right after impact and μ is the impulse ratio. When the coefficient of restitution is 0 and the impulse ratio is at a maximum (100 percent its critical value), the energy loss is a maximum. An impulse ratio at its maximum (when the relative tangential separating velocity is 0) occurs when both point of contact *P* on both vehicles obtain a common velocity during the impact phase. This is an important factor for this chapter. The results to the input found in table 1 using the momentum approach proposed by Brach [4] are shown in table 4-2.

Table 4-2: Output from momentum module

	Vehicle 1	Vehicle 2
V_x (mph)	2.813	16.786
V_y (mph)	-2.686	-8.714
Ω (deg per sec)	-248.378	12.697
ΔV (mph)	22.86	26.126

Energy loss (lbf-ft)	*PDOF* (deg)
173278.146	-82.933

$v_{cPbefore}$ (mph)	CV_x (mph)	CV_y (mph)
56.687	-20	54.641

Table 4-2 will be compared to the energy approach at a latter portion of Chapter 4. The upper case V represents the translational velocity of both vehicles after impact and the subscripts x and y correspond to their respective components. The upper case Ω represents the rotational velocity of both vehicles after impact. CV represents the closing velocity of both vehicles.

The Energy Module

It was mentioned in the objective of this chapter that, due to the difference in the approach to both methods, their input variables were different. The required input for the energy method can be categorized as follows: the energy dissipated during impact, the physical properties of the vehicles (masses and rotational inertias), the approach angle (heading of vehicle 2 toward vehicle 1) and the collision-damage characteristics (point of contact, direction of impact force, restitution coefficient, slip coefficient).

This research does not focus on the accuracy of the method used to calculate the energy dissipated during the collision, but the method proposed by Campbell [5] will be used. When good crush profiles are available, it is more dependable to estimate a value for the energy dissipated than to guess different initial velocities. On the other hand, if reliable energy data is not obtainable, the energy method will not give reliable results. The description of the energy module found below will describe how the energy and the point of impact *P* can be calculated from the damage profile of vehicle 1. Similar to the momentum module, both vehicles need the same three parameters to be graphically represented. Once the dimensions of the vehicle are specified, the damage profile can then be added. It is highly desirable, for the purpose of achieving accurate results, to enter actual measured damage dimensions whenever possible. The required dimensions for a complete definition of the damage are the width of the crushed region and the depth of the indentation. This module does not account for architectural incompatibility; therefore the value of the depth of indentation for a specific width cannot vary as a function of the height of the vehicle. An accurate average value for the variation in height must be estimated or calculated to best represent the crush depth as a single input

value. Figure 4-3 represents a frontal crush profile. The reference point for all frontal crush measurements is the front left hand corner of the vehicle. That point corresponds to the origin of the crush zone. At that point, the width is equal to zero and the crush depth is c_0 as defined in Figure 4-3. If no crush is visible at that point, c_0 has a value of 0 inches. It follows that the crush depth at width w_1 is c_1 and for the whole width

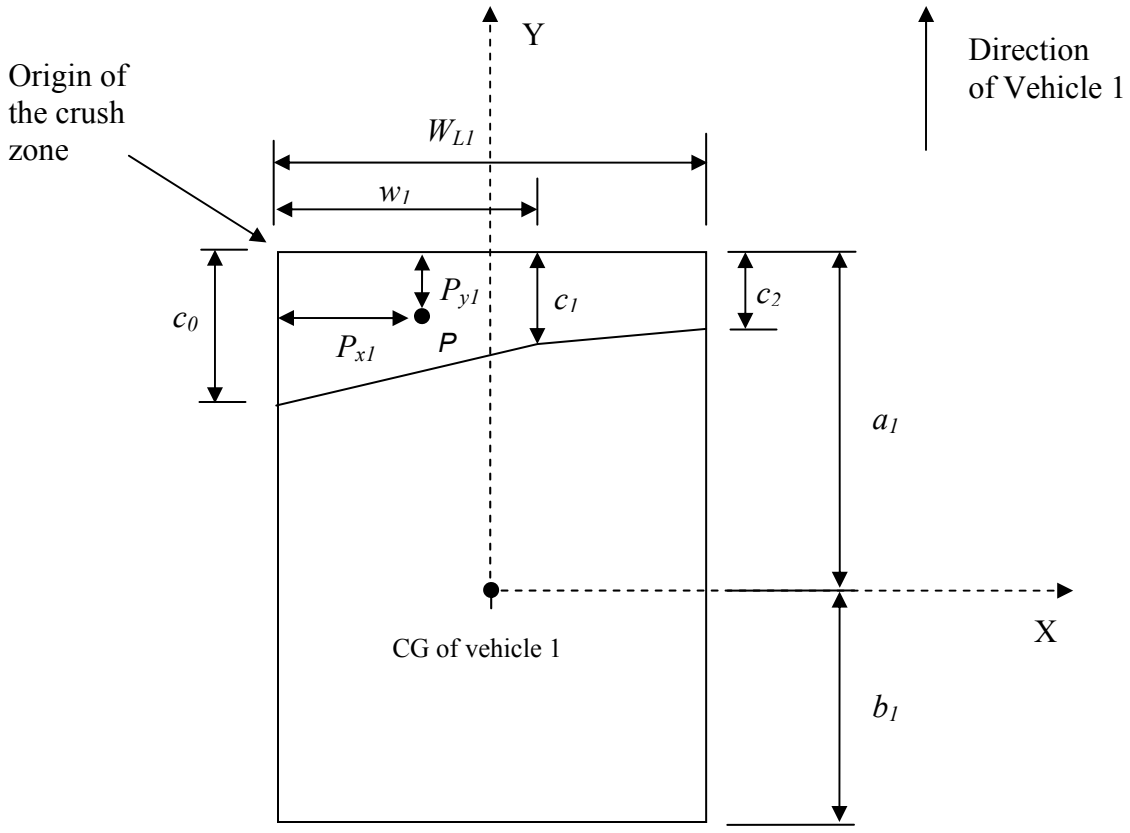

Figure 4-3: Frontal damage profile for vehicle 1

W_{L1}, its corresponding crush depth is c_2 in inches. Figure 4-3 only illustrates 3 different crush depths but the user is not limited to that representation. The module can be updated to more or less arguments according to the need of the user and the accuracy of the

known crush profile. The module can also be adapted for side and rear crush profiles. The measurements are specified in the form of an array as represented below:

$$C_1 = \begin{pmatrix} c_0 \\ c_1 \\ c_2 \end{pmatrix} \; in \qquad\qquad W_1 = \begin{pmatrix} 0 \\ w_1 \\ W_L \end{pmatrix} \; in \tag{4.5}$$

For a more general case:

$$C_1 = \begin{pmatrix} c_0 \\ c_1 \\ \vdots \\ c_{n-1} \\ c_n \end{pmatrix} \; in \qquad\qquad W_1 = \begin{pmatrix} 0 \\ w_1 \\ \vdots \\ w_{n-1} \\ W_L \end{pmatrix} \; in \tag{4.6}$$

n being the number of depth measurements.

The crush profile for vehicle 2 is independent of the angle of approach θ, therefore the same method is applicable to vehicle 2. Theoretically, during an impact two point masses come into contact at a single point on their outer surface area. If the masses are significantly small, that point of contact can represent their overall surface area. However, for a large stiff body (i.e. cars), the point of contact cannot be represented accurately as the center of area because only a portion of the surface area comes into contact. To simplify the analysis, it is suggested that the centroid (point *P*) which defines the geometric center of the projected area be used as the point of contact on each vehicle. This point could be adjusted by the user if better information is known. Given the projected crush depth matrix and its corresponding width matrix, the projected crush area can be calculated using the trapezoidal rule as shown in Equation 4.7.

$$Area_1 = \sum_{i=1}^{n1} \Delta a_{1i} \tag{4.7}$$

$$\Delta a_{1i} = \frac{1}{2}\left(C_{1i} + C_{1i+1}\right)\Delta w_{1i} \tag{4.8}$$

where the subscript *i* represents the ith row value of a vector.

$$i = 1\ ,\ 2\ \ldots\ n1 \quad \& \quad n1 = \left(\#\ of\ row\ of\ Crush_1 - 1\right)$$

$$\Delta w_{1i} = W_{1i+1} - W_{1i} \tag{4.9}$$

Once the projected area is calculated, the coordinates for the centroid of the projected area can be determined. The centroid for the surface area of an object such as a trapezoid plate, can be found by subdividing the area into simpler shapes (i.e. square or triangle) and computing the "moments" of these area elements about each of the coordinate axes. The width coordinate calculation for the point *P* is as follows:

$$P_{x1} = \frac{\sum_{i=1}^{n1} wpp_{1i}}{Area_1} \tag{4.10}$$

$$wpp_{1i} = wp_{1i}\ \Delta a_{1i} \tag{4.11}$$

$$wp_{1i} = W_{1i} + \Delta w_{1i}\left[\frac{C_{1i} + 2\ C_{1i+1}}{3\left(C_{1i} + C_{1i+1}\right)}\right] \tag{4.12}$$

Likewise, the depth coordinate calculation for the point *P* is as follows:

$$P_{y1} = \frac{\sum_{i=1}^{n1} cpp_{1i}}{Area_1} \tag{4.13}$$

$$cpp_{1i} = cp_{1i}\ \Delta a_{1i} \tag{4.14}$$

$$cp_{1i} = \frac{1}{2}\left[C_{1i} + \left(C_{1i+1} - C_{1i}\right)\frac{wp_{1i} - W_{1i}}{\Delta w_{1i}}\right] \tag{4.15}$$

As shown in Figure 4-3, the calculations for the centroid *P* are measured from the origin of the crush zone. While this approach is correct and acceptable, the origin of the crush

zone is not a good reference point. The origin of the crush zone is a function of the width of the car and such a parameter varies from one vehicle to another. In order to make the module applicable to all vehicles and comparable to the momentum module, it is preferable to use the center of gravity of the car as the origin for the location of point P. The new coordinates x_1 and y_1 are obtained from P_{x1}, P_{y1}, a_1, and W_{L1} as follows:

$$x_1 = P_{x1} - \frac{W_{L1}}{2} \tag{4.16}$$

$$y_1 = a_1 - P_{y1} \tag{4.17}$$

All calculations shown above for vehicle 1 are applicable to vehicle 2. However, for graphical reconstruction, all coordinates (of vehicle 2) are rotated by a rotation matrix about the z-axis illustrated by identity 4.18:

$$Rotation_{matirx} = \begin{pmatrix} cos(\theta) & -sin(\theta) \\ sin(\theta) & cos(\theta) \end{pmatrix} \tag{4.18}$$

In 1974, Campbell [5] estimated that the energy absorbed in plastic deformation could be determined using the damage dimensions and the dynamic force-deflection characteristics of the vehicle by expression 4.19.

$$E_1 = A_1\,\alpha_1 + B_1\,\beta_1 + \frac{A_1^{\,2}}{2B_1}\,L_1 \tag{4.19}$$

where

$$\alpha_1 = \sum_{i=1}^{n1}\left[\frac{1}{2}\left(C_{1i} + C_{1i+1}\right)\Delta w_{1i}\right] \tag{4.20}$$

$$\beta_1 = \sum_{i=1}^{n1}\left[\frac{1}{6}\cdot\left[\left(C_{1i}\right)^2 + C_{1i}\,C_{1i+1} + \left(C_{1i+1}\right)^2\right]\Delta w_{1i}\right] \tag{4.21}$$

$$L_1 = \sum_{i=1}^{n1}\Delta w_{1i} \tag{4.22}$$

His method used a linear approximation of the relationship between residual crush and impact speed (Figure 4-4). The values Campbell uses for the slope and intercept of the line are determined from frontal barrier impact test data for some different classes of cars. The coefficient *A* referred to as the spring preload and *B* as the spring constant per unit width are related to b_0 and b_1 of Figure 4-4 [5].

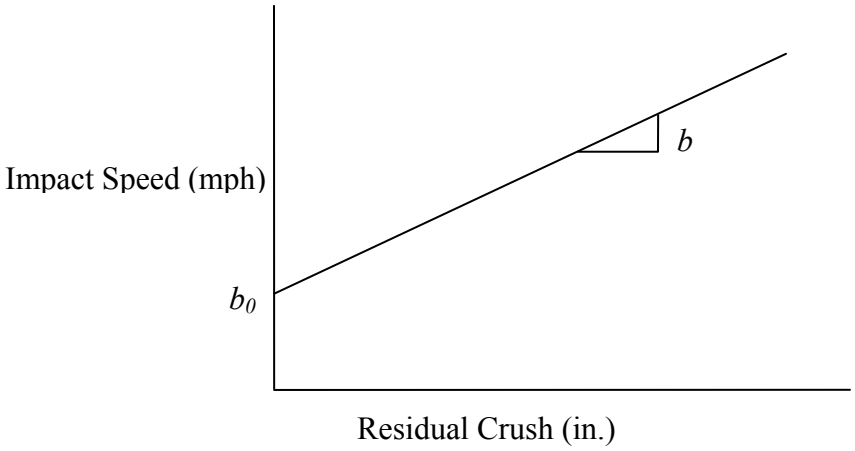

Figure 4-4: Plot of Residual Crush v.s. Impact Speed for Frontal Barrier Tests

Note that it is evident that the resolution of the energy calculation is proportional to the number of data point measured and the validity of the values for the coefficient *A* and *B*. In other words, more crush depth points per unit width will provide more accurate results. Also, a more detailed discussion of how to appropriately model crush energy can be found in [25]. The calculation for the crush energy for vehicle 2 will be similar to vehicle 1. The calculations shown above for the force and the crush energy are only correct in the condition that the force acts perpendicular to the front end of the car. Cases where the principal force is not perpendicular to the front end of the car will be discussed below.

Even though the force during impact is distributed over the damage area, the energy approach assumes that within the projected damage area of each vehicle exists a point *P* that has a force equal in magnitude and opposite in direction to the force exerted on the point *P* of the other vehicle. The angle θ_E represents the estimated direction of the force through the point *P*. Because it is a challenge to accurately estimate θ_E, its value can be changed to optimize the results. Recall that vehicle 1 is always heading along the y-axis. A positive value for θ_E is counter clockwise from the y-axis, and a negative value for θ_E is clockwise from y-axis. The energy calculation illustrated by expression 4.19 corresponds to a force of angle 0 deg. The adjusted energy calculation as a function of θ_1 is expressed by Equation 4.23.

$$EI_1 = E_1\left(1 + tan^2\left(\theta_E\right)\right) \tag{4.23}$$

If the direction of force does not pass through the center of the vehicle, the vehicle will be subject to rotation. The calculation for the value of the moment arm of the force relative to the CG of the car is as follows:

$$h_1 = x_1\ cos\left(\theta_E\right) + \ y_1\ cos\left(\theta_E\right) \tag{4.24}$$

Figure 4-5 gives a graphical representation of the significance of θ_E. If the angle of approach θ is a varying parameter and the module requires a value for the angle of the force on vehicle 1, by Newton's third law, θ_2 can be computed using the algorithm as follows:

$$\theta_2 = -\left[\pi - \left[\theta_E + \left(2\pi - \theta\right)\right]\right] \tag{4.25}$$

Similarly to vehicle 1, a positive value for θ_2 is counter clockwise from the heading of vehicle 2 and a negative value if clockwise from its heading. The adjusted energy

calculation as a function of θ_2 is expressed by Equation 4.26.

$$E2_2 = E_2 \left(1 + tan^2(\theta_2)\right) \tag{4.26}$$

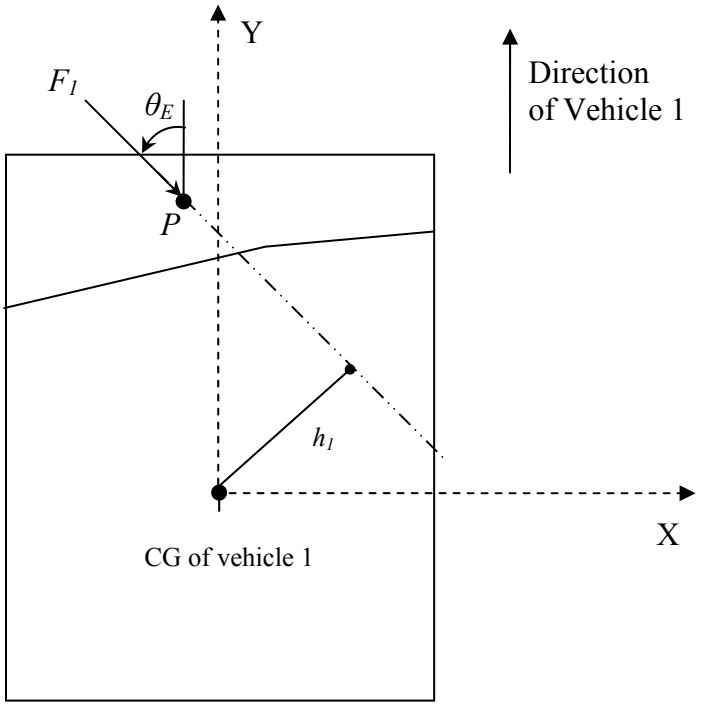

Figure 4-5: Direction of the force (Vehicle 1)

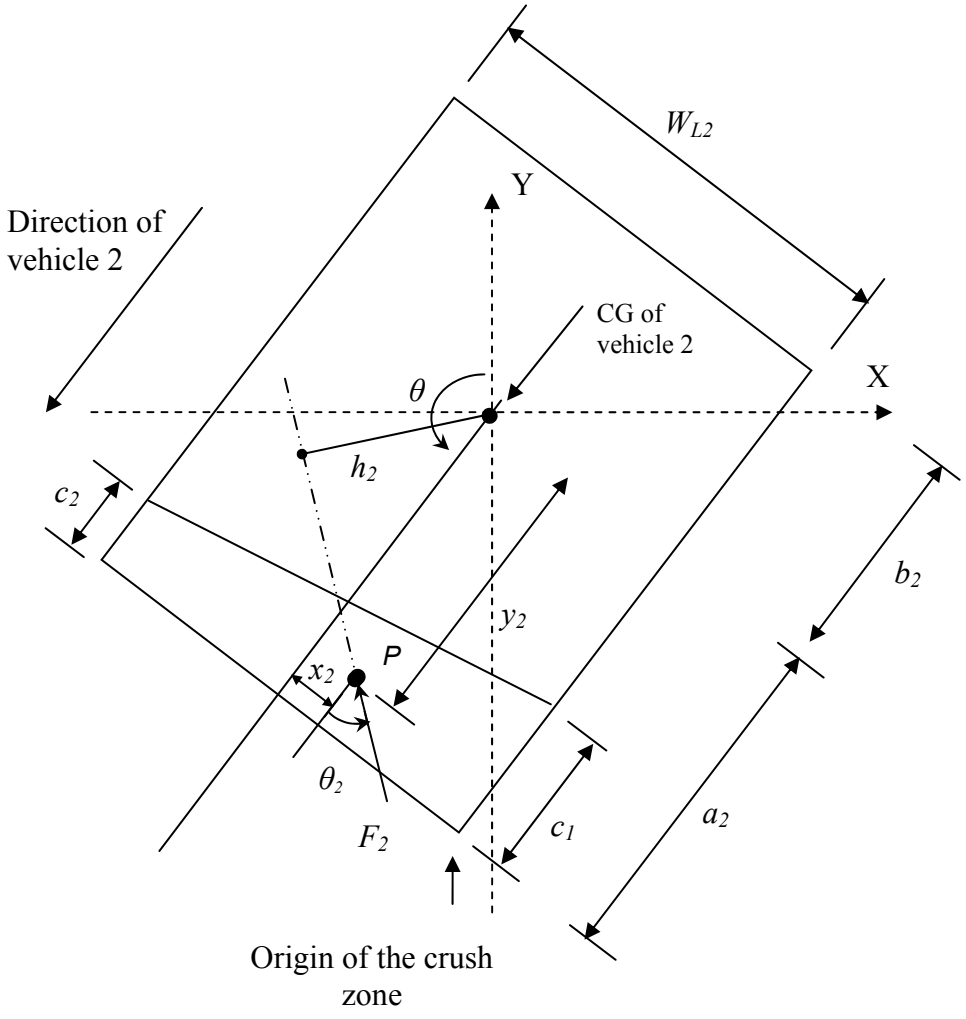

Figure 4-6: Direction of force (Vehicle 2)

The calculation for the value of the moment arm through the CG of vehicle 2 is as follows:

$$h_2 = x_2 \cos(\theta_2) + y_2 \cos(\theta_2) \tag{4.27}$$

Equation 2.12 is used to determine the closing velocity in the direction of F_1 once the masses and the rotational moment of inertia are specified. In addition, Equations 2.14 and 2.15 provided the change in velocities for both vehicles at point P. The change in

velocities at the CG of each vehicle can be obtained from the following expressions $\Delta V_1 = \gamma_1 \Delta V_{1P}$ and $\Delta V_2 = \gamma_2 \Delta V_{2P}$.

Pinned-Joint Constraint

In the case when there is no restitution and no sliding, the point *P* on each vehicle reaches a common velocity. We will show here how the change in velocities at the CG for both vehicles can be separated into their initial values, prior and after impact.

First it is critical to define the expression for the change in rotational velocity of each vehicle. If the angular velocity of both vehicles is 0 before impact, the change in rotational velocity can be reduced to the value of the rotational velocity after impact. If the value is negative, the angular velocity is represented counter clockwise. Likewise, if the value is positive, the angular velocity is represented clockwise. The angular velocities after impact are as follows:

$$\Omega_1 = \frac{\Delta V_{1P} - \Delta V_1}{h_1} = \frac{\Delta V_{1\omega}}{h_1} \tag{4.28}$$

$$\Omega_2 = \frac{\Delta V_{2P} - \Delta V_2}{h_2} = \frac{\Delta V_{2\omega}}{h_2} \tag{4.29}$$

The next step is to determine the components of the change in closing velocity for each vehicle in the x-y coordinate system. Consider Figure 4-7. Vehicle 1 is struck at point *P* by a force F_1 causing a positive rotational velocity Ω_1. Vehicle 1 is subject to two changes in velocity, one translational, ΔV_1 and one rotational and $d\Omega_1$. At this point it is possible to individually represent the two velocity vectors in their x and y

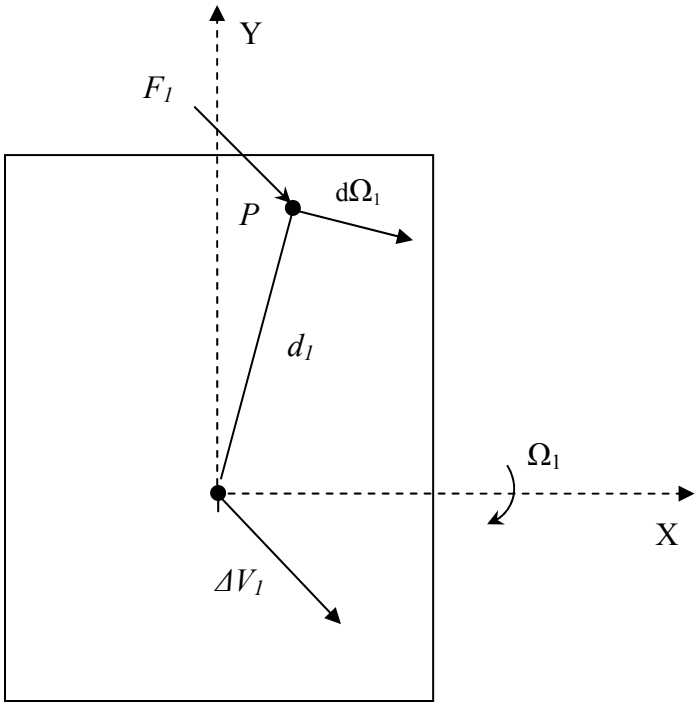

Figure 4-7: Translational components

components. The magnitude of ΔV_1 oriented by the angle θ_E in the x direction is determined using simple trigonometry as follows:

$$\Delta V_{1x} = \Delta V_1 \, sin(\theta_E) \tag{4.30}$$

Similarly the magnitude of ΔV_1 in the y direction is represented as follows:

$$\Delta V_{1y} = \Delta V_1 \, cos(\theta_E) \tag{4.31}$$

$d\omega_1$ represents the velocity at the point P due to rotation velocity of vehicle 1. Its magnitude and direction is calculated from Equation 4.32 shown as follows:

$$d\vec{\Omega}_1 = \vec{d}_1 \times \vec{\Omega}_1 \tag{4.32}$$

The x component of the change in closing velocity for vehicle 1 is the sum of expression 4.30, and the x component of 4.32 represented by Equation 4.33

$$CV_{1x} = \Delta V_{1x} + d\Omega_{1x} \tag{4.33}$$

The y component is the sum of expressions 4.31, and the x component of 4.32 represented by Equation 4.34.

$$CV_{1y} = \Delta V_{1y} + d\Omega_{1y} \tag{4.34}$$

A similar procedure can be followed for vehicle 2 to determine the x and the y components of the change in closing velocity. The value of θ_2 needs to be recalculated to adjust for the heading of vehicle 2. The expression for the new θ_2 is as follow:

$$\theta_2 = \theta_2 + \theta \tag{4.35}$$

The components of the change in closing velocity for both vehicle acting in the same direction can be subtracted to yield a value for each of the component of the closing velocity. The expressions for both components are shown in Equations 4.36 and 4.37.

$$CV_x = CV_{2x} - CV_{1x} \tag{4.36}$$

$$CV_y = CV_{2y} - CV_{1y} \tag{4.37}$$

As mentioned earlier, the velocities before impact will be represented by the lowercase v notation while the velocities after impact will be referred to by the uppercase V. Since the module forces vehicle 1 in the y direction, its initial velocity has no value in the x direction. Therefore the value of CV_x corresponds to the value of v_{x2}. Since

$v_{y2} = \frac{v_{x2}}{tan(\theta)}$, $v_{y1} = v_{y2} - CV_y$.

The calculations for the velocities after impact are more tedious to obtain because of the quadratic equalities 4.38 and 4.39. First consider the following equalities for vehicle 1:

$$\Delta V_1 = \sqrt{(v_{y1} - V_{y1})^2 + (v_{x1} - V_{x1})^2} \tag{4.38}$$

$$\theta_E = atan\left(\frac{V_{y1} - v_{y1}}{V_{x1} - v_{x1}}\right) \tag{4.39}$$

The system of Equations 4.38 and 4.39 can be solved but due to the quadratic nature of Equation 4.38, two set of solutions can be obtained for V_{x1} and V_{y1}. When θ_E is bound between -180 and 0 degrees, it will yield the corresponding set of solution. If θ_E is not within the bound, it will yield the second set of solution.

Now consider the following equalities for vehicle 2:

$$\Delta V_2 = \sqrt{\left(v_{y2} - V_{y2}\right)^2 + \left(v_{x2} - V_{x2}\right)^2} \tag{4.40}$$

$$\theta_E = atan\left(\frac{V_{y2} - v_{y2}}{V_{x2} - v_{x2}}\right) \tag{4.41}$$

Similarly, two sets of solutions can be obtained for V_{x2} and V_{y2}. When θ_E is bound between -180 and 0 degrees, it will yield the corresponding solution. Consider the scenario given in table 4.1. Table 4-3 is the rearranged list of input to satisfy the energy method. We substituted the initial velocities for the energy loss and the direction of the force found in table 4-2.

Table 4-3: Input for Energy module

	Vehicle 1	Vehicle 2
M (lb)	4000	3500
k (ft)	4.484	4.288
a (in)	80	80
b (in)	60	60
W_L (in)	80	80
θ (deg)	0	-150
x (in)	24	24
y (in)	60	60

Energy loss (lbf-ft)	ε	$PDOF$ (deg)
173278.146	0	7.067

Notice that the value of the *PDOF* output from table 4-2 is different than the *PDOF* input from table 4-3. The momentum module gave us the *PDOF* of the system from the x-axis but the energy method recognizes its value from the y-axis. $\frac{\pi}{2}$ is added to the momentum *PDOF* to satisfy the *PDOF* for the energy approach. The results are shown in table 4-4.

Table 4-4: Output from energy module

	Vehicle 1	Vehicle 2
V_x (mph)	2.813	16.786
V_y (mph)	-2.686	-8.714
Ω (deg per sec)	248.378	-12.697
ΔV (mph)	22.86	26.126
v (mph)	20	40

$v_{cPbefore}$ (mph)	CV_x (mph)	CV_y (mph)
56.687	-20	54.641

Beside a sign difference on the rotational velocity, the results are astounding. Using a number of decimal place to the 3rd order for both modules, every result matched exactly. The sign difference is a definition problem; the momentum module assumes left hand coordinate as positive and the energy method assumes right hand coordinate as positive. On the other hand, the calculations for the velocity prior and post impact are based upon the accuracy of the calculation of the closing velocity. The closing velocity is determined entirely from the heading angle of vehicle 2 toward vehicle 1 and the changes in velocities of both vehicles. Because we force the heading of vehicle 1 in the y direction, no solution can be obtained when vehicle 2 is aligned with vehicle 1. In such a case, the component of the closing velocity in the x direction is 0 and we are left with one equation and two unknowns.

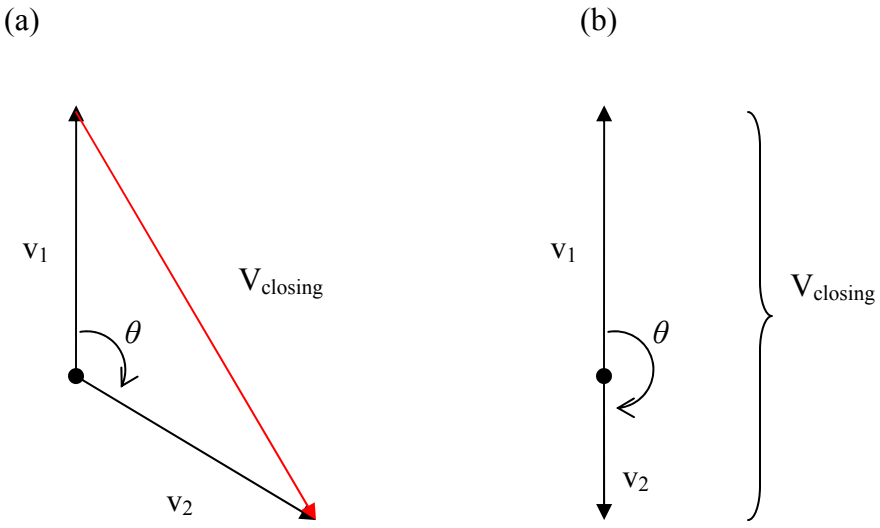

Figure 4-8: Closing Velocity when $\theta = -120$ (a), and $\theta = 180$ (b).

Therefore accurate results cannot be obtained when θ is chosen to represent a head-on or a rear-on collision. A variance of 1degree from those singular point cases can yield reasonable results. Figure 4-8 gives a graphical representation of a non singular and one of the singular point.

Velocity Ratio

θ_E is a difficult parameter to estimate using the energy approach and often its selected value is justified by the experience the reconstruction expert has. We will show how the direction of the force between two vehicles during impact can be accurately calculated if the ratio of their velocities prior impact can be estimated.

We showed in Chapter 4 that using the correct direction of the force on an appropriate contact point between two vehicles that are subject to no restitution nor sliding was enough to determine the direction of the closing velocity prior to impact. It follows that using the same energy approach, if the direction of the closing velocity were known before impact, the direction of force during impact could be determined accurately. Figure 4-8 illustrates graphically what the closing velocity represents. The heading angle of vehicle 2 toward vehicle 1 and the magnitude of each velocity are necessary to entirely define the closing velocity. However, the ratio $\frac{|\mathrm{v}_2|}{|\mathrm{v}_1|}$ along with the heading angle of v_2 toward v_1 are sufficient to specify the heading of the closing velocity. The components of the closing velocity can be calculated from expression 4.42 and 4.43.

$$\mathrm{CV}_x = \frac{|\mathrm{v}_2|}{|\mathrm{v}_1|} sin(\theta) \tag{4.42}$$

$$\mathrm{CV_y} = 1 - \left(\frac{|\mathrm{v_2}|}{|\mathrm{v_1}|} cos(\theta) \right) \tag{4.43}$$

Recall Equations 4.36 and 4.37. If a similar approach is used with the closing velocity in the direction of F_1 defined by Equation 4.44

$$\mathrm{CV_y}\ cos(\theta_E) - \mathrm{CV_x}\ sin(\theta_E) \tag{4.44}$$

there exist only one value for θ_E such that the value for expression 4.42 equals expression 4.36 and expression 4.43 equals expression 4.37. This method is valid as long as both vehicles experience a pinned-joint constraint during impact. This approach provides a reliable method to determine the direction of the force when the ratio of their velocities prior to impact is available or accurately estimated.

CHAPTER 5: PHYSICAL CONSTRAINTS AND BOUNDARY CONDITIONS

Objective

In Chapter 4, we introduced the first type of physical constraint that can take place during an accident. That physical constraint was expressed by forcing the point of impact *P* of both vehicles to have the same velocity. In other words, the 2 points remained connected and did not separate during impact. We also showed that the velocities prior and post impact for both vehicles for that first case could be determined. Unfortunately not all collisions can be represented by this pinned-joint constraint. In this chapter, we will present three additional cases for the energy module and we will identify under which conditions they are identical to the momentum approach. We will show how the velocities prior and post impact can be obtained from the changes in velocity. The first additional case represents two vehicles that experience restitution but are not allowed to slide during the impact. The second and third additional cases will introduce sideswipe impact with and without restitution. Additionally, plots of the velocities are provided to create a visual representation of their magnitude and directions as the parameter θ_E varies from 0 to 360 degrees.

Pinned-Joint Constraint with Restitution

In Chapter 8 of "Vehicle Accident Analysis and Reconstruction Methods" [4], the authors specify the limitations of the CRASH3 model. They affirm that results are valid

as long as "the collision is perfectly inelastic, that is, there can be no rebound or restitution of the vehicles at and perpendicular to the crush surface" [4]. In the case when a restitution coefficient is introduced, the results will only be consistent between both approaches when the n-axis of the momentum is aligned with the *PDOF* of the energy module. This hypothesis is logical since the restitution in the energy module is specified in the direction of F_1 and along the n-axis for the momentum module. What does a coefficient of restitution physically represent and how does it affect the calculations to obtain the velocity prior and post impact? Consider a coefficient of restitution of 0.15. Such a coefficient of restitution states that an additional fifteen percent of the velocity prior to impact is imparted to the velocity after impact. The assumption that the point *P* on each vehicle has the same velocity is no longer correct because the vehicles bounce apart during impact. However, the method used in Chapter 4 to calculate the closing velocity components can still be used as long as the relative velocity of both points *P* due to the separating velocity is accounted for. The separating velocity is the product of the closing velocity with the coefficient of restitution. Therefore, this separating velocity term can directly be subtracted from the changes in velocity at the center of gravity of either one of the vehicles. Equations 5.1 and 5.2 are used to replace Equations 4.30 and 4.31. The magnitude of ΔV_1 oriented by the angle θ_E in the x direction can be redefined as follows:

$$\Delta V_{1x} = \left(\Delta V_1 - \varepsilon v_{cPbefore}\right) sin\left(\theta_E\right) \tag{5.1}$$

Similarly the magnitude of ΔV_1 in the y direction is represented as follow:

$$\Delta V_{1y} = \left(\Delta V_1 - \varepsilon v_{cPbefore}\right) cos\left(\theta_E\right) \tag{5.2}$$

Notice that when $\varepsilon = 0$, expressions 5.1 and 5.2 become expression 4.30 and 4.31 subsequently. Using Equations 5.1 and 5.2 inside of 4.36 and 4.37 satisfies both the pinned-joint constraint and the pinned joined constraint with restitution.

Consider the scenario depicted by table 5-1.

Table 5.1: Input for momentum module

	Vehicle 1	Vehicle 2
M (lb)	4000	3500
k (ft)	4.484	4.288
a (in)	80	80
b (in)	60	60
W_L (in)	80	80
θ (deg)	0	90
x (in)	24	-24
y (in)	60	60
v (mph)	10	35
ω (deg per sec)	0	0

θ_1 (deg)	ε	μ
-61.946	0.15	100% μ_0

Table 5-2 shows the results of Table 5-1 using the momentum module.

Table 5-2: Output from momentum module for ε = 0.15

	Vehicle 1	Vehicle 2
V_x (mph)	-13.07	-20.063
V_y (mph)	3.035	7.96
Ω (deg per sec)	214.873	-45.373
ΔV (mph)	14.81	16.925

Energy loss (lbf-ft)	*PDOF* (deg)
59908.387	-151.946

$v_{cPbefore}$ (mph)	CV_x (mph)	CV_y (mph)
35.591	35	10

Table 5-3 is the rearranged list of input to satisfy the energy method.

Table 5-3: Input for Energy module

	Vehicle 1	Vehicle 2
M (lb)	4000	3500
k (ft)	4.484	4.288
a (in)	80	80
b (in)	60	60
W_L (in)	80	80
θ (deg)	0	90
x (in)	24	-24
y (in)	60	60

Energy loss (lbf-ft)	ε	*PDOF* (deg)
59908.387	0.15	-61.946

The results of Table 5-3 using the energy module are shown in table 5-4.

Table 5-4: Output from energy module for ε = 0.15

	Vehicle 1	Vehicle 2
V_x (mph)	-13.07	-20.063
V_y (mph)	3.035	7.96
Ω (deg per sec)	-214.873	45.373
ΔV (mph)	14.81	16.925
v (mph)	10	35

$v_{cPbefore}$ (mph)	CV_x (mph)	CV_y (mph)
35.591	35	10

The results for both modules are identical. This approach will always be consistent as long as the *PDOF* for the energy module is aligned with the value chosen for the n-axis of the momentum module.

Sideswipe Impact

Another limitation of the CRASH3 model found in Chapter 8 of "Vehicle Accident Analysis and Reconstruction Methods" [4], is that results are valid as long as "the relative sliding velocity of the vehicles along (tangent to) the crush surface ends (becomes zero) before or at the time the vehicles separate" [4]. A sideswipe collision occurs when the vehicles continue to slide over the contact surface throughout the contact duration. In the momentum module, the critical impulse ratio μ_o is calculated when no relative tangential velocity at end or prior to separation at point *P* of each car exists. By definition when $\mu = \mu_o$, no sliding exists and when $|\mu < \mu_o|$ sliding exists at separation. The absolute value sign is necessary because the sign of μ determines the direction of the tangential impulse. A convenient way of handling the selection of a

value of μ is to express it as a percentage of μ_o that ranges between 0% and 100%. In the energy model, Equation 2.11 is the critical equation that governs the impulse of the system. It is valid for any collision (including sideswipe) as long as all of the values are accounted for in the direction of the force. For the pinned-joined case, the separation velocity at point *P* is 0, therefore Equation 2.11 became Equation 2.12 with $\varepsilon = 0$. Written in different form Equation 2.12 can be represented by Equation 5.3.

$$v_{cP\,before} = \sqrt{\frac{2E_R}{M_{eff}} + v_{cP\,after}{}^2} \tag{5.3}$$

When sliding or restitution is introduced to the system, the separating velocity in the direction of the force needs to be added and the impulse of the system changes. This point is illustrated graphically using Figure 5-1. Let V_s be the sliding velocity vector along the t-axis and V_r be the restitution velocity vector along the n-axis. The separating velocity, $V_{separating}$ is the resultant of those two vectors. The direction of the force is defined by the value of the adjusted impulse ratio μ.

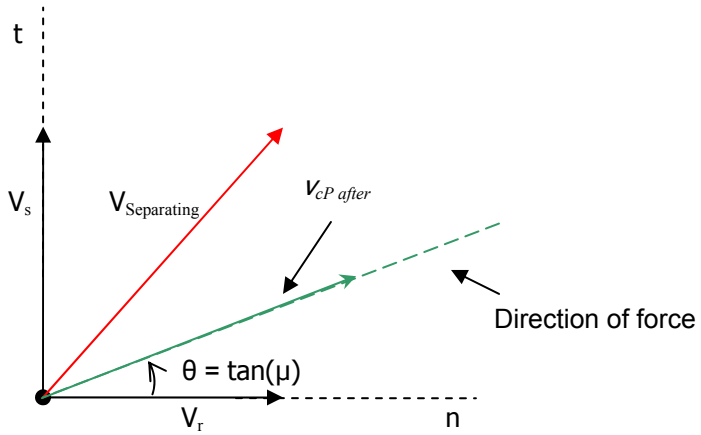

Figure 5-1: Representation of the separating velocity in the momentum module.

As mentioned above, it is clear that if V_s and V_r are 0, $V_{separating}$ is also 0 and Equation 2.12 is valid. That situation represents a pinned-joint constraint. When V_s is 0, $V_{separating}$ is V_r and that situation is representative of a pinned-joint constraint with restitution. For this case, V_r is 0 so $V_{separating}$ is V_s. Because the format of Equation 2.12 changed, Equations 2.14 and 2.15 also need to be redefined. They are replaced by Equations 5.4 and 5.5.

$$\Delta V_{1P} = \left(v_{cP\,befpre} - v_{cP\,after}\right)\frac{M2_{eq}}{M2_{eq} + M1_{eq}} \tag{5.4}$$

$$\Delta V_{2P} = \left(v_{cP\,before} - v_{cP\,after}\right)\frac{M1_{eq}}{M1_{eq} + M2_{eq}} \tag{5.5}$$

As seen with the pinned-joined case with restitution, the method used in Chapter 4 to calculate the closing velocity components can also be used when sliding is present. The separating velocity components due to sliding can directly be subtracted from the changes in velocity at the center of gravity of either one of the vehicles. Equations 5.6 and 5.7 are used to replace Equations 5.1 and 5.2. The magnitude of ΔV_1 oriented by the angle θ_E in the x direction can be redefined as follow:

$$\Delta V_{1x} = \Delta V_1 \, sin\left(\theta_E\right) - \mathrm{V}_{\mathrm{separation_x}} \tag{5.6}$$

Similarly the magnitude of ΔV_1 in the y direction is represented as follow:

$$\Delta V_{1y} = \Delta V_1 \, cos\left(\theta_E\right) - \mathrm{V}_{\mathrm{separation_y}} \tag{5.7}$$

where $\mathrm{V}_{\mathrm{separation_x}}$ and $\mathrm{V}_{\mathrm{separation_y}}$ are the components of Equation 5.9. In order to compare results between both models, we will use the momentum model to assume a third arbitrary scenario. The components of the separating velocity of point *P* and the

magnitude of the separating velocity in the direction of the force will be calculated from the momentum model and used as an input for the energy model. In Chapter 3, we used Equation 3.11 to determine the velocity after impact from the change in velocity and the velocity before impact. Similarly, the velocity after impact for point *P* of each vehicle can be written as follows:

$$v_{P1after} = \Delta V_{1P} + v_{P1before} \tag{5.8}$$

where $\Delta V_{1P} = \Delta V_1 + \Delta V_{1\omega}$ from Equation 2.24. Because both vehicles are assumed to not have rotational velocities before impact, the velocity of point *P* on each vehicle before impact is the velocity of their center of gravity. The changes in velocity due to angular rotation after impact can be seen from Figure 4-6.

Table 5-5: Input for momentum module for $\mu = 80\% \mu_o$

	Vehicle 1	Vehicle 2
M (lb)	2600	2000
k (ft)	4.975	4.912
a (in)	80	80
b (in)	60	60
W_L (in)	80	80
θ (deg)	0	110
x (in)	30	-30
y (in)	70	70
v (mph)	10	51
ω (deg per sec)	0	0

θ_1 (deg)	ε	μ
253	0	80% μ_0

The velocity after impact of point *P* for vehicle 2 and for vehicle 1 can be reduced to a set of x-y components and the difference between each component in their respective axis defines the separating velocity components.

$$V_{\text{separation}} = v_{P2\,after} - v_{P1\,after} \tag{5.9}$$

Once the critical impulse ratio is calculated, it is adjusted to simulate sliding conditions. In addition to the energy dissipated and the *PDOF* corresponding to the adjusted impulse ratio, the magnitude of the separating velocity in the direction of the *PDOF* ($v_{cP\,after}$ in Equation 5.3) is used as an input for the energy model. Notice that the equations found in this sideswipe impact case encompass all the equations for the previous two cases.

Consider the scenario chosen in table 5-5. Table 5-6 shows the results of Table 5-5 using the momentum module. Table 5-7 is the rearranged list of input to satisfy the energy method. The results are shown in table 5-8. The results for both modules are identical.

Table 5-6: Output from momentum module for $\mu = 80\% \mu_o$

	Vehicle 1	Vehicle 2
V_x (mph)	-12.88	-31.18
V_y (mph)	0.204	-4.708
Ω (deg per sec)	171.951	48.136
ΔV (mph)	16.182	21.037

Energy loss (lbf-ft)	*PDOF* (deg)
92149.233	-142.744

$v_{cPbefore}$ (mph)	CV_x (mph)	CV_y (mph)
54.758	47.924	27.443

$v_{cPafter}$ (mph)	$Vseparation_x$ (mph)	$Vseparation_y$ (mph)
10.76	3.876	12.677

Table 5-7: Input for energy module

	Vehicle 1	Vehicle 2
M (lb)	2600	2000
k (ft)	4.975	4.912
a (in)	80	80
b (in)	60	60
W_L (in)	80	80
θ (deg)	0	110
x (in)	30	-30
y (in)	70	70

Energy loss (lbf-ft)	ε	*PDOF* (deg)
92149.233	0	-52.744

$v_{cPafter}$ (mph)	$Vseparation_x$ (mph)	$Vseparation_y$ (mph)
10.76	3.876	12.677

Table 5-8: Output from energy module

	Vehicle 1	Vehicle 2
V_x (mph)	-12.88	-31.18
V_y (mph)	0.204	-4.708
Ω (deg per sec)	-171.951	-48.1
ΔV (mph)	16.182	21.037
v (mph)	10	51

$v_{cPbefore}$ (mph)	CV_x (mph)	CV_y (mph)
54.758	47.924	27.443

Sideswipe Impact with Restitution

The calculations and the approach for a sideswipe impact with restitution are identical to the sideswipe impact discussed above. As shown in Figure 5-1, the momentum module presented by Brach [4] provides restitution in the direction of the n-axis and slip along the t-axis. When calculating the separation velocity along the direction of the *PDOF* from the momentum model, both components to both axes are accounted for. Equations 5.6 and 5.7 along with Equations 4.36 and 4.37 are still valid. Table 5-9 and 5-10 represent the solution to both module of the scenario presented in table 5-5 with a coefficient of restitution on 20%. Once again the results are identical.

Table 5-9 Output from momentum module for $\varepsilon = 0.2$ and $\mu = 80\%\ \mu_o$

	Vehicle 1	Vehicle 2
V_x (mph)	-14.476	-29.106
V_y (mph)	0.062	-4.524
Ω (deg per sec)	202.36	76.563
ΔV (mph)	17.559	22.826

Energy loss (lbf-ft)	*PDOF* (deg)
92556.657	-145.53

$v_{cPbefore}$ (mph)	CV_x (mph)	CV_y (mph)
55.042	47.924	27.443

$v_{cPafter}$ (mph)	$Vseparation_x$ (mph)	$Vseparation_y$ (mph)
5.606	-3.375	14.822

Table 5-10 Output from energy module for $\varepsilon = 0.2$

	Vehicle 1	Vehicle 2
V_x (mph)	-14.476	-29.106
V_y (mph)	0.062	-4.524
Ω (deg per sec)	-202.36	-76.563
ΔV (mph)	17.559	22.826
v (mph)	10	51

$v_{cPbefore}$ (mph)	CV_x (mph)	CV_y (mph)
55.042	47.924	27.443

Plots of Velocities as a function of θ_E from 0 to 360 degrees

As addressed earlier, the energy method requires two parameters in its model that are very difficult to accurately assess by only looking at the residual crush of two

impacted vehicles. Using these parameters as variables, the model algebraically obtains values for estimated changes in velocity at a point *P* relative to the crushed energy dissipated during the impact. Even though the value for the two varying parameters (the angle θ_1 representing the estimated direction of the force at impact through the point *P* of vehicle 1 and the angle θ at which vehicle 2 approaches vehicle 1) can individually be changed, the outcome of the module will only represent the results for those individually changed values. A graphical representation of the results as a function of a varying abscissa can be useful for two reasons. First, they provide a physical meaning for the results and whether these results are reasonable or not. Second they allow the user to accurately define the correct value of the direction of the force, θ_E, given the accident scene provides additional information. Information such as the heading of vehicle 1 after impact, the heading of vehicle 2 after impact, the closing velocity heading or the separating velocity heading. It is not suggesting that such information is always obtainable from any given accident, but knowing one of them would be sufficient to back-track θ_E as seen in Figures 5-2 or 5-3. Notice that this approach is valid for all four cases with different constraints.

Consider the following scenario. $M_1 = 2600\ lb$, $M_2 = 2000\ lb$, $k_1 = 4.975\ ft$, $k_2 = 4.912\ ft$, $x_1 = 30\ in$, $y_1 = 70\ in$, $x_2 = -30\ in$, $y_2 = 70\ in$, $\theta = 110\ deg$, $\varepsilon = 0$, and, $E_R = 1\ lbf\text{-}ft$.

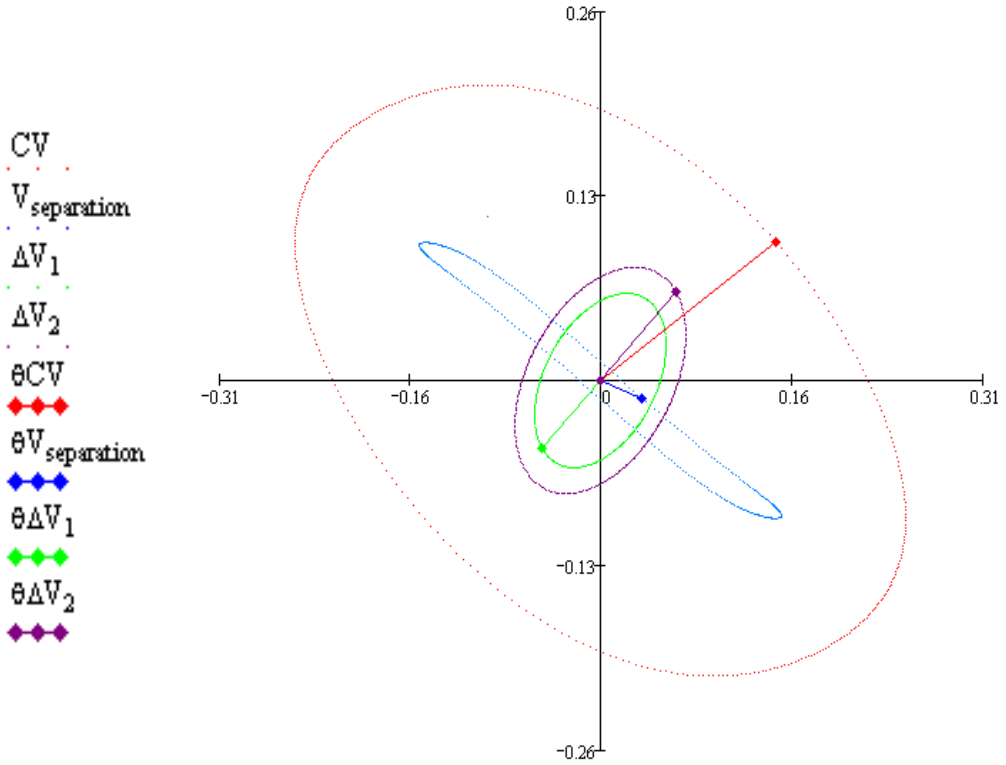

Figure 5-2: Plot of velocities difference as a function of θ_E from 0 to 30 degrees

Figure 5-2 shows the closing velocity, the separating velocity and the changes in velocity of vehicle 1 and vehicle 2 in the direction of θ_E as a function of θ_E from 0 to 360 degrees. For a given value of θ_E, the corresponding results are represented by the solid vector lines. For the scenario depicted in Figure 5-2, the specific value of θ_E is -45 degrees. Figure 5-3 shows the velocities prior and post impact for vehicle 1 and vehicle 2 as a function of θ_E from 0 to 360 degrees. For the specific value of θ_E used in Figure 5-2, the corresponding results are represented by the solid vector lines.

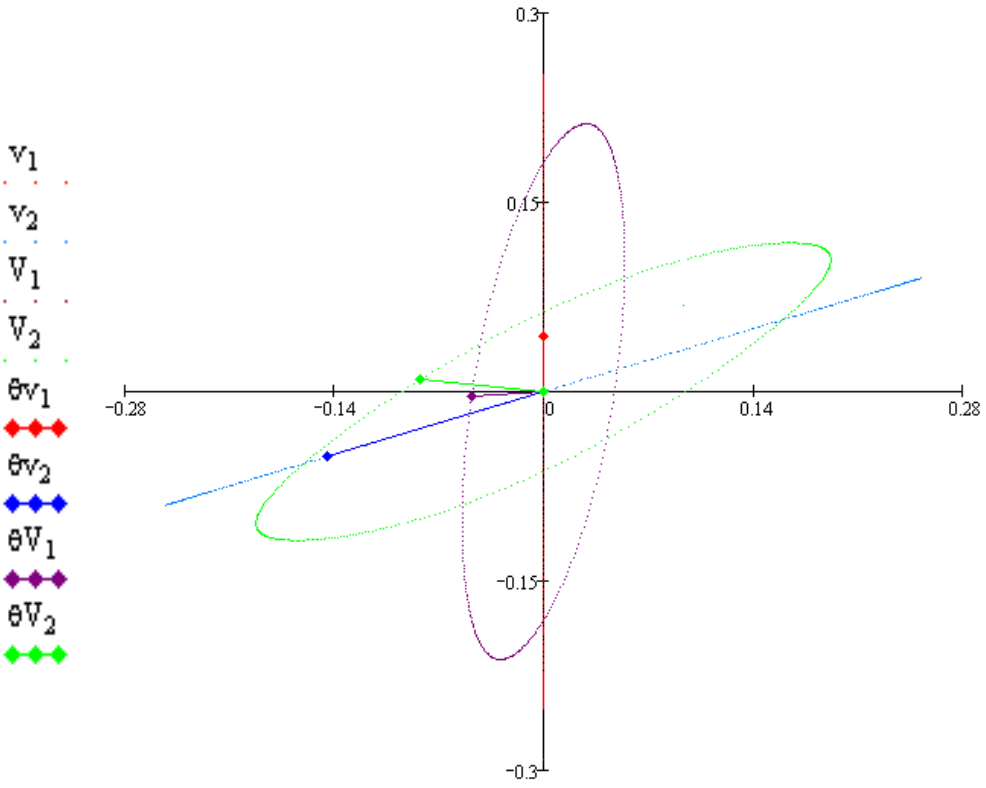

Figure 5-3: Plot of velocities as a function of θ_E from 0 to 360 degrees

As mentioned in Chapter 3, the energy dissipated during the impact does not affect the direction of the velocities but rather it is needed to scale their magnitude. Each plot updates as the user varies θ.

CHAPTER 6: CONCLUSION

Objective of the Paper

The objective of this paper is threefold. First, create a general energy model to reconstruct the impact phase in automobile collision. Second, non-dimensionalize the model and determine all the power impulses from the energy dissipated. Third, establish a constituent approach to show that a momentum approach model [4] is identical to this general energy model for any given scenario.

New Insight for Both Approaches

It is apparent from the work shown above that both methods can provide identical results to any given scenario when using the correct set of inputs. One method is not considered better than the other; neither can it be said that one method is more accurate than the other. Both methods have their set of different assumed input but they also share similar input. The conclusion is the following: both methods should be used in any given scenario but the scenario that provides the more accurate set of inputs will yield more accurate results to its corresponding method.

Contributions

It is evident that accident reconstruction has been subject to much research over the last 40 years and there have been a lot of papers and articles written. This thesis

contributes added insight into the two current methods of reconstructing the impact phase of a collision. The energy method has been redefined in a more general approach and the energy dissipated during the collision is used as an impulse in power to identify the changes in energy propagated into both vehicles. The limitation of the CRASH3 solution to calculate the changes in velocity have been studied and extended to allow sideswipe and restitution to be accounted for. In addition to the revised assumptions, a method was developed to accurately separate the velocity prior to and post impact for both vehicles from their changes in velocity. Finally, different methods to consistently determine the direction of the force are presented when additional information from the accident scene is provided.

REFERENCES

1. Brach, R. Matthew., et al., "Crush Energy and Planar Impact Mechanics for Accident Reconstruction," 980025, SAE.

2. Brach, Raymond M., "Least Squares Collision Reconstruction," 870429, SAE.

3. Brach, Raymond M., et al., "A Review of Impact Models for Vehicle Collision," 870048, SAE.

4. Brach, Raymond M., et al., Vehicle Accident Analysis and Reconstruction Methods, SAE, 2005.

5. Campbell, Kenneth., "Energy Basis for Collision Severity," 740565, SAE.

6. Carpenter, Nicholas J., et al., "Stiffness and Crush Energy Analysis for Vehicle Collision and its Relationship to Barrier Equivalent Velocity (BEV)," 2001-01-0500, SAE.

7. Cliff, William E., et al., "Validation of PC-Crash – A Momentum-Based Accident Reconstruction Program," 960885, SAE.

8. Day, Terry D., et al., "Application and Misapplication of Computer Programs for Accident Reconstruction," 890738, SAE.

9. Fay, Richard Fay., et al., "PC-Crash and HVE, an Overview of Similarities and Differences," 2001-01-0505, SAE.

10. Germane, Geoffrey J., et al., "Introduction of Pulse Shapes and Durations into Impulse-Momentum collision Models," 2005-01-1183, SAE.

11. Ishikawa, Hirotoshi., "Impact Center and Restitution Coefficients for Accident Reconstruction," 940564, SAE.

12. Long, Timothy J., "Introduction of the Barrier Equivalent Time (BET) Methodology in the Analysis of Delta-V," 2000-01-0462, SAE.

13. McHenry, Raymond R., "A Revised Damage Analysis Procedure for CRASH Computer Program," 861894, SAE.

$X_{vehicle2}$

14. McHenry, Raymond R., et al., “Effects of Restitution in the Application of Crush Coefficients,” 970960, SAE.

15. Neptune, James A., “Crush Stiffness Coefficients, Restitution Constants, and a Revision of CRASH3 & SMAC,” 980029, SAE.

16. Neptune, James A., et al., “Impact Analysis Based Upon the CRASH3 Damage Algorithm,” 950358, SAE.

17. NHTSA, “CRASH-3 User’s Guide and Technical Manual”, U.S. Department of Transportation, National Highway Traffic Safety Administration, Washington, D.C. 29590.

18. Robinson, Edward L., “Derivation of Closing Speed as a Function of Dissipated Energy,” 2000-01-1318, SAE.

19. Rose, Nathan A., et al., “Crush and Conservation of Energy Analysis:Toward a Consistent Methodology,” 2005-01-1200, SAE.

20. Rose, Nathan A., et al., “Restitution Modeling for Crush Analysis: Theory and validation,” 2006-01-0908, SAE.

21. Smith, Gregory C., “Conservation of Momentum Analysis of Two-Dimensional Colliding Bodies, With or Without Trailers,” 940566, SAE.

22. Smith, Russell A., and al., “Accuracy and Sensitivity of Crash,” DOT HS - 80 -152, NHTSA.

23. Steffan, Hermann., et al., “The Collision and Trajectory Models of PC-CRASH,” 960886, SAE.

24. Swider, Piotr., et al., “SMASH – Program for Car Accident Simulation,” 2000-01-0848, SAE.

25. Woolley, Ronald L., “Non-Linear Damage Analysis in Accident Reconstruction,” 2001-01-0504, SAE.

26. Woolley, Ronald L., et al., “ An Overview of Selected Computer Programs for Automotive Accident Reconstruction,” TRB subcommittee A3B 11 (02).

27. Woolley, Ronald L., et al., “Inaccuracies in the CRASH3 Program,” 850255, SAE.